THE ANALYSIS OF IONOSPHERIC DRIFT MEASUREMENTS

by

C.E. MEEK

February, 1978

Institute of Space and Atmospheric Studies
Physics Department
University of Saskatchewan
Saskatoon, Canada

ACKNOWLEDGEMENTS

I would like to thank Louine Schnell and Alice Brown for helping with some of the more painful data analysis.

ABSTRACT

Various methods for reducing D region partial reflection drift measurements to wind values are discussed. Criteria for comparing the quality of deduced winds from different analyses, as well as for choosing suitable records for analysis are defined. These are used to compare some data from different locations. Possible systematic biases in wind value and related parameters due to the type of analysis, antenna coupling, data averaging, or ionospheric conditions (e.g. shear) are also evaluated.

THE ANALYSIS OF IONOSPHERIC DRIFT MEASUREMENTS

by

C.E. MEEK

February, 1978

Institute of Space and Atmospheric Studies
Physics Department
University of Saskatchewan
Saskatoon, Canada

TABLE OF CONTENTS

TABLE OF CONTENTS- cont'd

TABLE OF CONTENTS- cont'd

TABLE OF CONTENTS- cont'd

LIST OF FIGURES- cont'd

LIST OF FIGURES

LIST OF FIGURES- cont'd

LIST OF TABLES

CHAPTER I

INTRODUCTION

This report is based on work done during research on a Ph.D. project (Meek,1977) involving a comparison of partial reflection winds and electron densities. Since most of the useful results arose from an investigation of winds measurement, it was decided to prepare a separate report on this aspect which would incorporate the results appearing in the thesis along with other work not included for reasons of 'balance' and pertinence to the research topic. The report has been built around Chapter 3, Appendix C, and Appendix D from the thesis.

Chapter 2 briefly summarizes results from a report on wind determination written prior to the thesis (Gregory and Meek, 1976), and should be read after Chapter 3 (sections 3.1-3.3) which provides an introduction to winds analysis methods. The rest of Chapter 3 deals with practical difficulties in local data, quality criteria which can assess and compare different locations, equipment, and analyses; and the development of a full correlation analysis, FCA, based on Fedor(1967), which is suitable for use on our data. Chapter 4 discusses several of the interesting records encountered during the course of the work. Most of these would not have led to a calculation of wind under normal analysis, but some useful data can be retrieved manually. Chapter 5 compares pattern parameters from U of S (Saskatoon, 52°N, 107°W), Ottawa, and Adelaide data. Chapter 6 discusses the effect of antenna coupling on

the calculated drift and pattern parameters. Appendix A contains a variety of topics expanding some comments made in the text, and is referred to by footnotes. Appendix B compares the effect on the computed FCA parameters of small changes in analysis, e.g. amount of data averaging. Appendix C describes practical details of the chosen FCA method. The added section, C.9, gives representative quantities and qualities of data for day and night conditions locally. Appendix D describes a method for 'exact' calculation of FCA parameters using the maximum value in each cross correlation and the width of the mean auto correlation. An added section, D.4, compares pattern parameters and quality of drift values between this, and the least squares fit method (Appendix C) which uses several points in each cross correlation. Appendix E evaluates the effect on the calculated FCA parameters of systematic modification of the auto and cross correlation information, whether due to the method of extracting numerical values, or to actual modification (e.g. smoothing, or averaging, of the original fading records).

The variety of subjects covered does not lend itself to a single concluding chapter.

As the original chapter on equipment has been left out, a brief description is given here. Figure 1.1 shows the present U of S antenna system. Usually north-south linear polarization is used in both receiving and transmitting antennas. Pairs of parallel dipoles in each receiving square are connected in

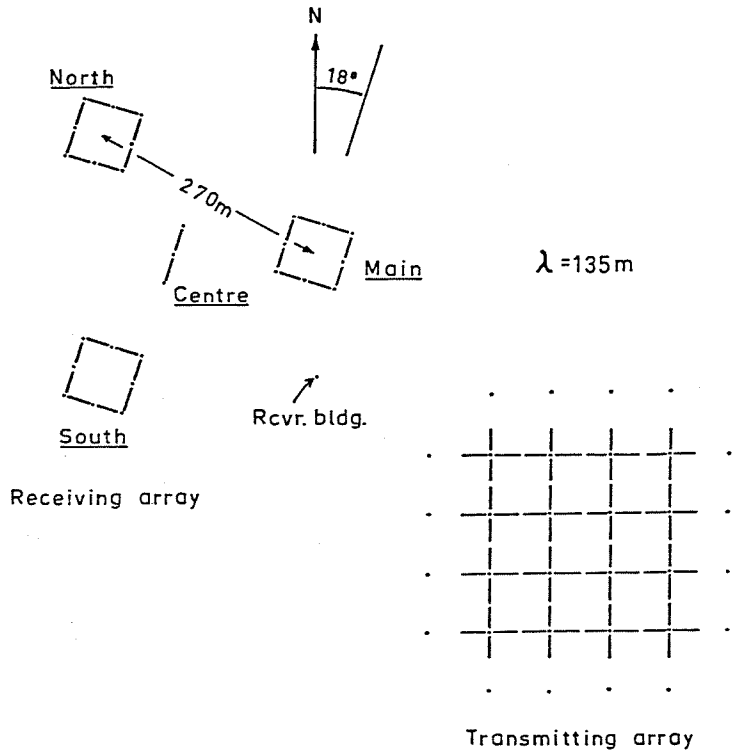

Figure 1.1 Antenna system (Saskatoon)

parallel. The operating technique is to switch one antenna into the receiver, send out a transmitter pulse (usually 20 s), and measure the instantaneous received signal at 23 delays (height gates) which correspond to scatter from 23 heights (usually 52-118 Km). Then the next antenna is switched in, and the process repeated. Amplitudes are recorded digitally on magnetic tape. The switching rate is usually 15 Hz., and some data averaging is done to reduce the number of samples in each amplitude sequence when the records are analysed. Auto and cross correlations between sequences are calculated up to some maximum lag for three pairs of antennas at a given height gate. The position, in lag, of peaks in the cross correlations represent 'average' pattern delays between antennas.

As can be seen from the antenna diagram, the ground amplitude is not sampled at points, but each sample represents a kind of average over the area of each antenna; the 'capture' area is larger than the physical dimensions. It would be interesting to estimate the effect of this averaging on the calculated drift velocity. It may be similar to that of low pass filtering discussed in Appendix E. However, since the statistics of point amplitudes are not directly measurable, the results of such a study would only give a general indication of the effects.

The 'small triangle' or 'small spacing' on our equipment refers to a simulated small triangle created by correlating pairs of fading sequences from the centre and one of the outer

antennas. Since the spacing of these pairs is equal, the 'small triangle' is equilateral and rotated by 30^{o} when compared to the 'large triangle' (which consists of just the outer antennas).

CHAPTER II

SUMMARY OF RESULTS FROM C.R.C. REPORT

2.1 Introduction

This chapter gives a brief summary of results appearing in a C.R.C. (Communications Research Centre, Ottawa) contract report (Gregory and Meek, 1976) which preceeded the thesis. The work was basically a comparison between methods then in use at U of S, and that at C.R.C. These were analyses for apparent velocity. For those unfamiliar with drifts analysis, comments made in this chapter will be more understandable after a reading of Chapter 3, sections 3.1-3.3.

2.2 Analysis methods.

The C.R.C. method, developed by M.J. Burke, was to split the fading sequences into short segments, analyse each segment for apparent velocity, and average the resulting vectors. He had chosen the segments by selecting single fading features (maxima) in each sequence, and dividing the data accordingly. Selection of single fading features was facilitated by smoothing the data beforehand. However, the method was modified for the report to divide the data into ~10 equal segments (per 5 min record). Also, two sample methods were tried. One of these averaged the velocity vectors resulting from analysis of each segment (a least squares fit of the apparent velocity to the time delays for maximum cross correlation was employed, with no rejection of data[1]). The other averaged the cross correl-

1. see Appendix A, section A.1

ations, and calculated one apparent velocity vector from these (rejection similar to the old U of S analysis, see section 3.3.1, was used). These two methods are called the average sample vector, and the average sample correlation respectively. The old U of S method, which correlated the full sequences (5 min) and then found apparent velocity from the location of cross correlation peaks, was compared to these. Since U of S data are very different in character (more difficult to interpret) from C.R.C. data, comparsion of analyses was restricted to C.R.C. data.

2.3 Results of the comparison

An initial test on smoothed data (13 point binomial filter on amplitude samples spaced at 1 second intervals, i.e. approximately a 5 sec running average) showed that the consistency of velocity values were much worse (as were the NTD values) than that of unsmoothed data. For example, for cross correlations of the full 5 min record, 60% of the unsmoothed data records had an NTD<0.1, compared to only 35% for the smoothed data. Pairs of wind vectors (old U of S analysis) at the same height, but separated in time by 5 min were examined for consistency. For the unsmoothed data, 80% of the angle differences were less than 30°, compared to 60% for the smoothed data. Consequently, analysis of smoothed data was not pursued any further.

Comparison of the consistency (as above) between the sample methods, and direct analysis (U of S) of the 5 min records showed that the latter was best, followed by the average sample

correlation; and the average sample vector method was worst. Other findings are noted below.

2.4 Other results and conclusions.

1) In the course of the work, a variety of operating parameters had been tried at U of S, including O-mode transmission and reception (normally we use linear), 50μsec pulse (normally20μsec), and longer (8 min) records (normally 3.2 min), with no apparent difference in NTD distribution.

2) Lower correlation peaks (median 0.25) had been found in U of S than in C.R.C. (median 0.4) data. This was at least partly due to our greater antenna spacing (270 m) compared with that at C.R.C. (169 m).

3) The fading rate (found from the width of the auto correlation) was found to be higher at U of S than at Ottawa, for as yet unexplained reasons. This is further discussed in Chapter 5.

4) Comparison of parabolic and Gaussian curve fitting to find the maxima in the cross correlations (exact fits to three points) was made. The major differences occur when peaks are close to zero lag, of course, and the lag step should be chosen so that the largest delay is not affected by differences in curve fitting. For some analyses (e.g. the PMFCA, Appendix D) the peak value of correlation is also important. This is poorly determined if the widths of the cross correlation peaks (which depend on the drift velocity and pattern parameters) are comparable to the lag step. It appears that the C.R.C. lag step

(1 sec) which is also the sample rate, is near (if not greater than) the maximum suggested value. Their antenna spacing is 169 metres, and the recommended maximum lag step can be scaled up or down according to this. Practical considerations restrict the choice of arbitrarily small lag steps since this requires higher sample rates (and thus more interference to other radio users) and more computation time to determine the cross correlations out to a suitable maximum delay. At present (U of S) we are obtaining fairly good results with a lag step of 0.533sec (which is also the sample rate) in conjuction with an antenna spacing of 156 metres.

5) When sample vectors (over a period of 40 min) with NTD>0.2 were discarded, the remaining vectors when plotted seemed to fall on a circle (e.g. Pütter, 1955) for some low heights (~60-70 Km). This would be expected if each sample corresponded to a single 'line of maximum' crossing the antenna system with a more or less random orientation and a constant drift velocity. This effect has not been found by other workers, who used time delays measured directly from similar fading features seen in amplitude-time graphs, but has been confirmed by M.J. Burke (private communication).

6) The C.R.C. equipment measured amplitudes at three antennas simultaneously, whereas U of S equipment cycles around the antennas (only one receiver required). Simultaneous measurement has the advantage of fewer required transmitted pulses (i.e. less interference to other users) but the disadvantage that

any interference (static) received will occur simultaneously in all three fading sequences; thus creating high cross correlations at zero lag. This effect can be seen in C.R.C. data when the signal level is low, but is generally not a problem. The noise level of the receiving site will be the determining factor. Of course, any continuous interference from outside radio transmissions is serious for both types of measurement, and may lead to spurious wind values. Cyclic interference (e.g. teletype) harmonically related to the cyclic measurement rate is also serious.

Some quantitative comparisons between U of S and C.R.C. data are in the following chapters and appendices.

CHAPTER III

WINDS THEORY AND ANALYSIS

3.1 Introduction

Much work has been done in the past on the analysis of fading records from spaced antennas, in order to estimate bulk motions of the neutral atmosphere at ionospheric heights. The fading pattern on the ground is caused by the reflection of radio waves from irregularities in electron density which are assumed to be carried along by the neutral wind.

There has been some argument, based on the nature of the scattering process and ground pattern, over the best type of analysis to use, and the relation of the computed drift vector to the neutral wind. Some workers (e.g. Briggs et al.,1950; Fedor,1967; Wright,1974) have assumed that the scattering is from a 'random screen' of irregularities, and that suitable statistical models may be used to estimate such parameters as drift velocity, average shape, and time change of the pattern. Others (e.g. Pfister,1971; Hines and Rao,1968; Felgate and Golley,1971; MacDougall,1966; M.J.Burke, private communication) have emphasized the wavelike nature of the pattern, at least for E and F region echoes. Felgate and Golley found that the D region partial reflections (Adelaide) were of the 'random screen' type.

Probably the truth lies between these two, since spectra of fading sequences generally have a roughly Gaussian shape (maximum at low frequencies) with minor peaks indicating enhanced energy at some discrete frequencies[1].

1. see Appendix A, section A.2

Some of these differences in opinion may arise from differing ionospheric conditions at different locations. For example, the winter fading rate at Ottawa was found to be lower than that at Saskatoon (U of S). There are differences in the quality of data as well, apparently not due to equipment or analysis factors. Fortunately, the absolute values of the wind are not as important in the present work as the directions, about which there seems to be no dispute.

The comparison of winds and electron densities required good quality winds data over short term periods; ideally each calculation producing an accurate value of wind. The existing analysis was found wanting in this respect. Previous use of the data had usually involved hourly averages (Manson et al.,1974; Gregory and Manson,1975) for determining seasonal changes. Reasons for the unacceptable number of poor values will be discussed later.

In the development of better analyses, some definitions of quality were required for the comparison of various methods. The first of these is the distribution of the normalized time discrepancy, a parameter to be defined later, which is available from each fading measurement, and is more a test of equipment, location, and preliminary data handling, than analysis method. Two dimensionless quantities which check the consistency of the final drift values are the angle difference ($\Delta\phi$), and the ratio of the magnitudes of the vector difference and sum (denoted $\Delta V/V$) for two vectors. These are defined in

Figure 3.1.

The distribution of these quantities, defined from pairs of adjacent drift vectors in height or time, can be used to indicate quality if the actual wind is assumed to vary relatively slowly. Some of the differences in quality between data gathered at different research establishments may be related to this assumption. A difficulty is that isolated wind determinations, remaining after obviously bad data have been discarded, and which are thus more likely to be spurious themselves, are not accounted for in the distributions. If the wind is assumed constant over long periods of time then the variance in values could be used for comparison; however the probable existance of real short term perturbations due to gravity waves reduces the usefulness of this type of test.

The rest of the chapter is an approximately 'historical' account of the various intermediate analyses tried, and comparison of these with others' experimental data. This was necessary because the data presented in the thesis had come from several different analyses. The priority in the development of a suitable analysis has been the internal consistency of data in routine processing rather than the accuracy of values with respect to actual neutral motion. The latter requires comparison with independent experiments (e.g. rocket observations), and it is possible that an analysis which compares well at one location may either be biased, or

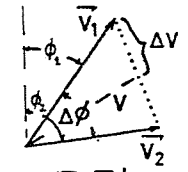

$$\frac{\Delta V}{V}=\frac{|\vec{V}_1-\vec{V}_2|}{|\vec{V}_1+\vec{V}_2|}\ ,\ \Delta\phi=|\phi_1-\phi_2|$$

Figure 3.1

Definition of the two dimensionless quantities used to measure consistency of wind values

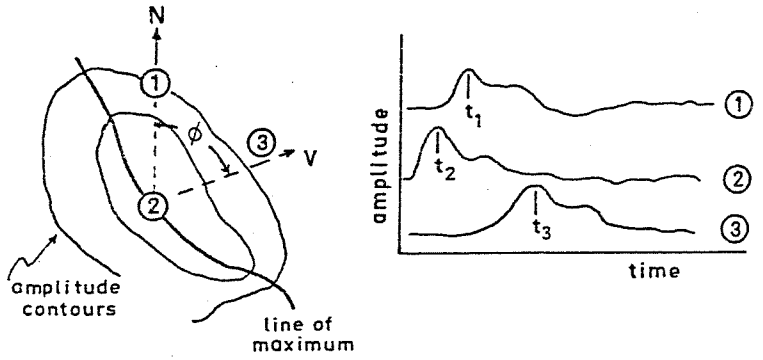

Figure 3.2 Illustration of a pattern feature crossing an antenna array, and the resultant fading records.

Figure 3.3

Illustration of an isometric pattern crossing an antenna array, and the sampled points in the pattern for each antenna.

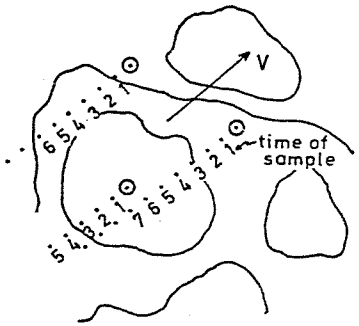

unusable at another because of differences in the ionosphere.

3.2 Similar fades analysis

This method (e.g. Mitra,1949) was used before computers became available, and consisted in examining fading sequences from three spaced antennas for similar features. The delays between antennas were used to calculate the drift velocity. Figure 3.2 illustrates a pattern crossing the antenna array (usually equilateral, or right angle isoceles) and the resulting amplitude sequences. The time delays are $t_{ij} = t_j - t_i$ where t_{ij} is positive if the pattern moves from antenna i to antenna j.

The normalized time discrepancy (N.T.D.) is defined as

$$\text{N.T.D.} = |\, t_{12}+t_{23}+t_{31}\,| \;/\; (\,|t_{12}|+|t_{23}|+|t_{31}|\,) \qquad ..(3.1)$$

and is identically zero in this case whether the line of maximum, shown in Figure 3.2, is curved, or changing in time. If the line of maximum is linear, perpendicular to the drift vector, and travelling at the drift velocity, then the correct value of drift is obtained from the time delays. These assumptions are not liable to hold for every line of maximum and so the time delays, or calculated drift vectors, are averaged over many fades (Sprenger and Schminder,1969). This is called the apparent velocity because internal pattern time change and non-isometric patterns (i.e. preferred directions of elongation) are not accounted for.

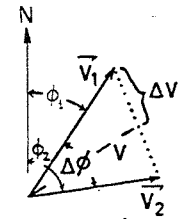

$$\frac{\Delta V}{V} = \frac{|\vec{V}_1 - \vec{V}_2|}{|\vec{V}_1 + \vec{V}_2|}, \quad \Delta\phi = |\phi_1 - \phi_2|$$

Figure 3.1

Definition of the two dimensionless quantities used to measure consistency of wind values

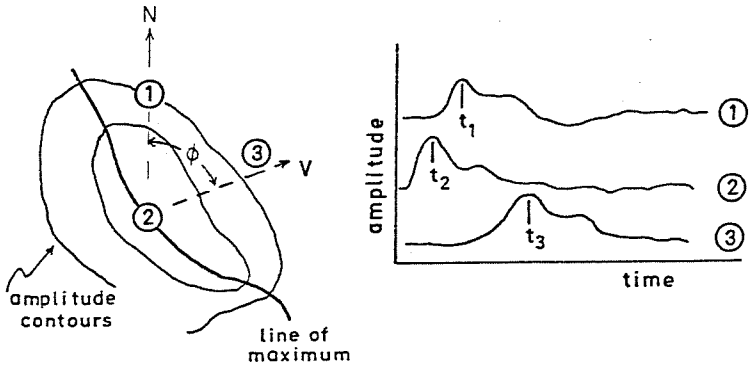

Figure 3.2 Illustration of a pattern feature crossing an antenna array, and the resultant fading records.

Figure 3.3

Illustration of an isometric pattern crossing an antenna array, and the sampled points in the pattern for each antenna.

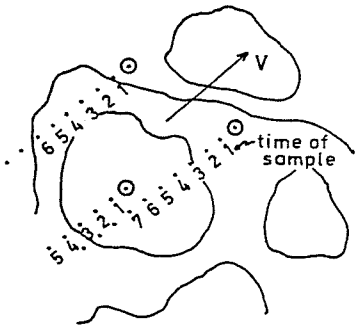

There are methods which claim to be able to overcome these difficulties by using the variance of the time delays over many individual fades (Briggs and Spencer,1955;Bamgboye et al.1974). However, computers are not ideally suited for the pattern recognition involved in the identification of similar fading features, and so correlation methods were developed.

3.3 Correlation methods (apparent velocity)

The computer equivalent to similar fades uses cross correlations between amplitude sequences recorded at different antennas. The location of the maximum cross correlation value in lag will define some sort of average delay in pattern occurrence between antennas. If the line of maximum concept is put aside, a better explanation of the usefulness of the cross correlation sequences can be made. Suppose that the pattern is isometric, i.e. statistically the same in any direction, and time invariant except for the drift motion. Figure 3.3 shows this situation. Then it can be seen that if the lags between amplitude sequences are such as to correspond to the time delay between antennas of a straight line, perpendicular to the drift, moving with the pattern, there will be a maximum in cross correlation because amplitudes at closest spatial separation in the pattern are being correlated. Thus, under these assumptions (and more generally, as will be shown later), the N.T.D. computed from the time delays for maximum cross correlation corresponds to that of the perpendicular line, and should be zero. Also the computed velocity will be correct.

3.3.1 Old U of S analysis

The old analysis computed the cross correlation sequences, ρ_{12}, ρ_{23}, ρ_{31}, to a maximum lag of 18 sec (about 10% of the amplitude sequence length). An accurate estimate of the position of the maximum value in each correlation was found by curve fitting. If the maximum value occurred at maximum lag, or was less than 0.1, the data were rejected. The N.T.D. distribution is shown in Figure 3.4 (see Table 3.1 for pertinent details of equipment and analysis) and compared with that for Ottawa (Communications Research Centre). The latter analysis did not reject any data, except for lack of signal, and used a comparatively larger maximum lag (20 sec) when the smaller spacing of the antennas is considered. Also shown is the distribution for Adelaide (A.H. Manson, private communication) after ~10% of the data had been rejected for various reasons. If the Adelaide curve is shifted down by ~10% it is similar to that for Ottawa, but U of S data are seen to be much worse. A baseline for comparison (dashed line) is the N.T.D. distribution for times which are uniformly distributed random values over the fixed maximum lag. The disparity between these data may depend to some extent on the height range sampled, and this variation will be shown in a later figure (but for smaller antenna spacing).

Under the old analysis the data were edited by a complicated set of criteria which were essentially equivalent to rejection if N.T.D. ≥ 0.7, and rejection of unreasonably high speeds. Two time delays are sufficient to define the pattern

Table 3.1 Equipment and analysis parameters for data plotted in Figures 3.4 to 3.8

Location	Freq. (MHz)	Ant. spacing (m)	Pulse width (sec)	mode	Record length (min)	Record spacing (min, Km)	sampled region (Km)	# pts./ seq.	Data avg.	Maxlag (sec)	Analysis	curve Fig. 3.4	curve Fig. 3.5-3.8
U of S	2.22	270	20	linear	3.2	5,3	52-118	960	3	18	Old UofS	b	b
"	"	"	"	"	"	5,1.5	64-97	"	"	"	Manual(V_a)	-	h
"	"	"	"	"	"	5,3	52-118	"	"	9	Old UofS	-	g
"	"	"	"	"	"	"	"	"	"	9(var)	FCA	o	o
"	"	156	"	"	"	"	"	760	2	6(var)	FCA	d	d
Ottawa	2.66	169	50	0-mode	5	5,2	44-98	300	-	20	Old UofS	e	e
Adelaide	2.4	~190	30	linear	3	3,2	81-99	846	2	7.6	FCA	f	f

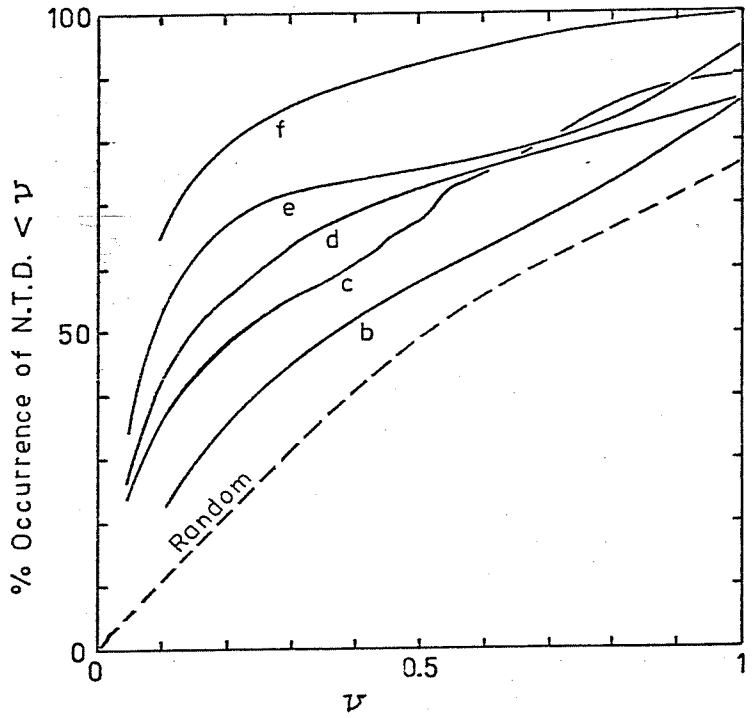

Figure 3.4 Distribution of the N.T.D. for U of S (b,c,d), Ottawa (e),and Adelaide (f). Further information is given in Table 3.1.

velocity according to the following equations (U of S geometry, e.g. Figure 3.2).

$$\left.\begin{aligned} t_{12} &= -\frac{d}{V_a}\cos\phi_a \\ t_{23} &= \frac{d}{V_a}\cos(60^\circ-\phi_a) \\ t_{31} &= -\frac{d}{V_a}\cos(120^\circ-\phi_a) \end{aligned}\right\} \qquad \ldots(3.2)$$

where d is the antenna spacing, and the drift angle, ϕ_a, is measured to the East from North. The three speeds, defined by pairs of time delays, were each required to be less than 500 m/s, and the median vector (in angle) was then used to represent the pattern velocity, which is divided by 2 to give the drift.

Distributions of $\Delta\phi$ and $\Delta V/V$ for height and time differences are shown in Figures 3.5 to 3.8 (curve b) and compared with Ottawa data analysed by the same method (curve e) and full correlation analysis (to be explained later) values from Adelaide (only in Figures 3.5 and 3.6, curve f). The rest of the plotted distributions will be explained later. Random distributions (dashed lines) are also shown. That for $\Delta\phi$ is just a uniform distribution over 0-180°. If the separate components of the vectors are taken to be independent, normally distributed random values with zero mean and equal variance, then $(\Delta V/V)^2$ posseses an F distribution with degrees of freedom $\nu_1, \nu_2 = 2$. Values for this distribution are available in statistical tables.

The experimental results show, for example, that only 36% of U of S adjacent-time vector pairs have angle differences less than 30° compared with 79% in the Ottawa data. The

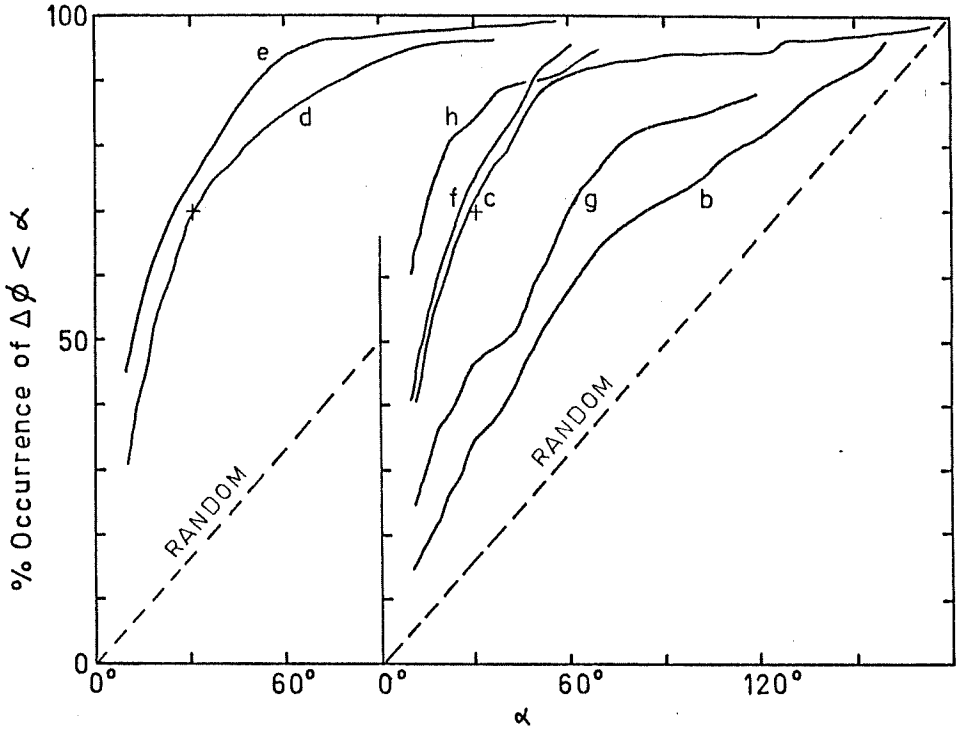

Figure 3.5 $\Delta\phi$ distribution for adjacent height vectors; U of S (b,c,d,g,h); Ottawa (e); Adelaide (f). '+' is a reference mark. Further information is given in Table 3.1.

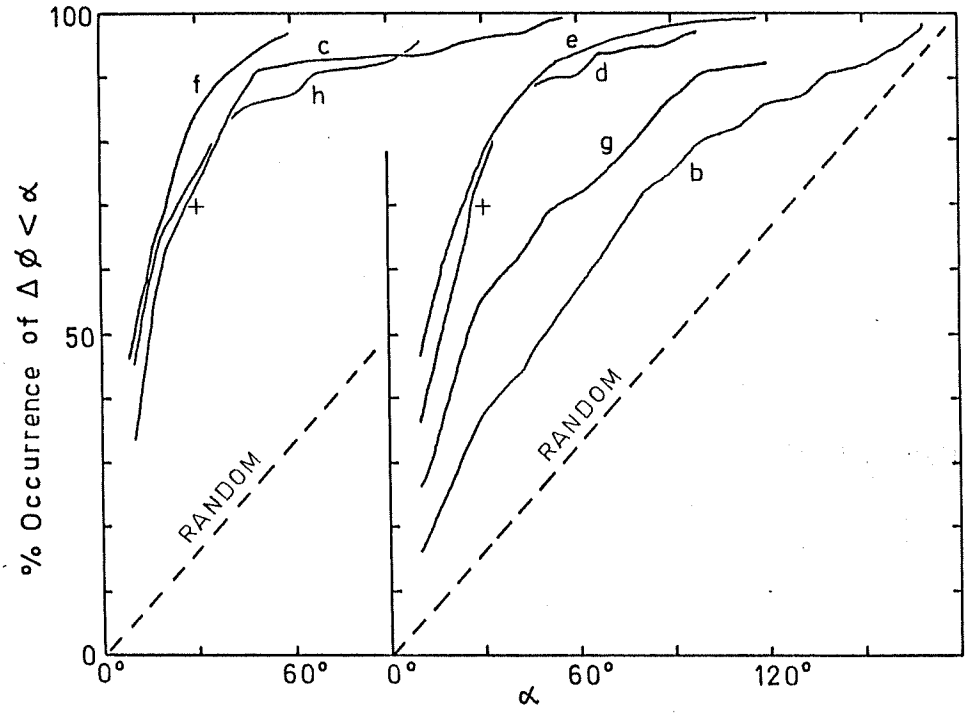

Figure 3.6 As in Figure 3.5, but for adjacent time vectors.

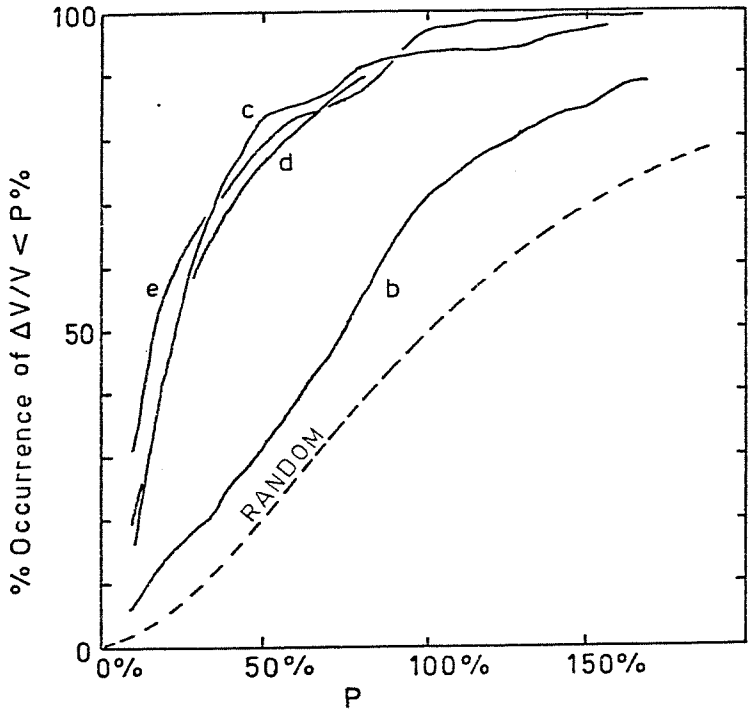

Figure 3.7 ΔV/V distribution for adjacent height vectors; U of S (b,c,d); Ottawa (e). Further information is given in Table 3.1.

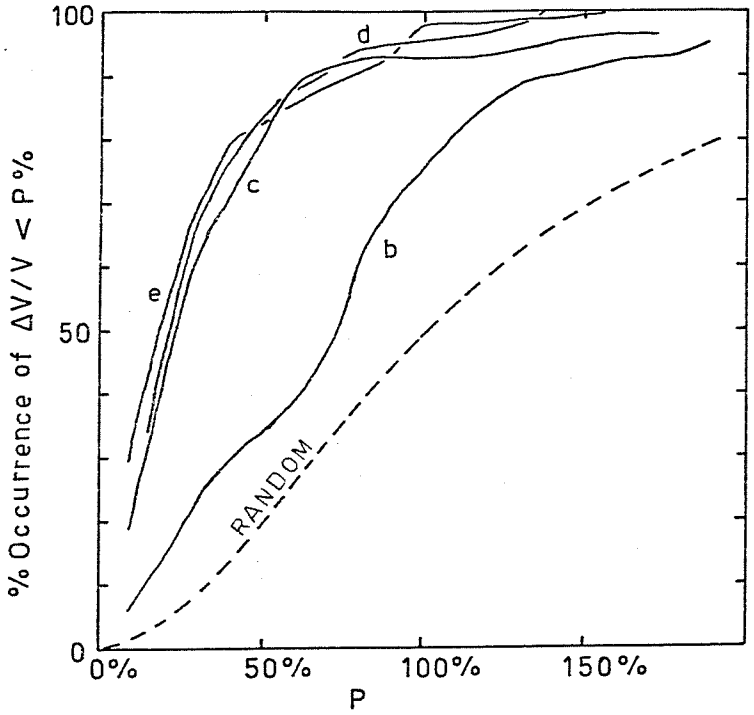

Figure 3.8 As in Figure 3.7, but for adjacent time vectors.

difference in quality is rather distressing , but it might have been expected from comparison of the N.T.D. distributions: because, although theoretically there is no direct connection between the two, they are closely related in practice.

3.3.2 Reasons for the disparity in quality

Further investigation showed that the 'correct' peaks in the cross correlation sequences are generally lower in our data than in that for Ottawa , at least partly due to our greater antenna spacing, and that there are a lot of spurious peaks. This then is at least a partial explanation for the difference in N.T.D. distributions, viz. the 'wrong' peaks are chosen more often. Possible explanations for these extra peaks include interference patterns, superposition of two pattern motions due to a strong shear in wind within the sample range (3 Km), or a change in wind during the record. In the latter two situations there would be a set of peaks for each drift motion. However, these possibilities are very difficult to test in routine analysis, and the present aim is to avoid these types of records. Some examples are shown in Figure 3.9 with the 'correct' peaks (based on minimum N.T.D.) arrowed. These have been chosen specifically to illustrate cases in which a secondary peak in a cross correlation is probably the correct one.

Another source of difficulty, prevalent in U of S data, but also present in Ottawa data as evidenced by their effects on the cross correlation sequences, are sudden jumps in

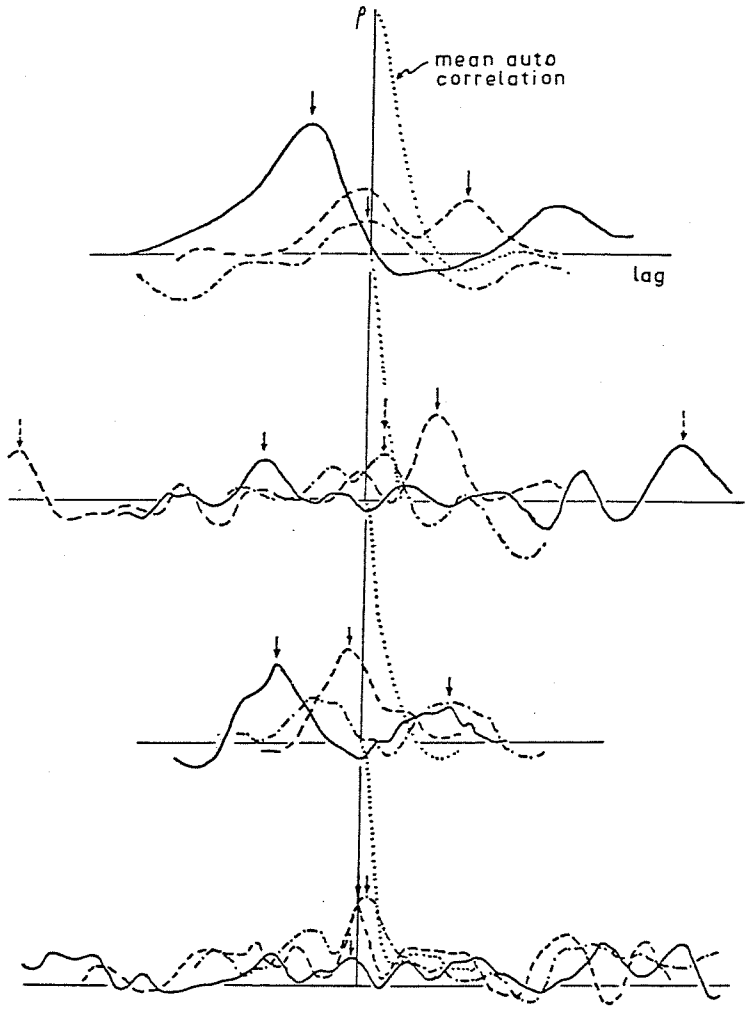

Figure 3.9 Examples of cross correlations for records in which a secondary peak could be chosen to make N.T.D.≃0. Chosen peaks are arrowed.

amplitude lasting as long as ~30 sec. These have been attributed to meteor trails, and generally occur above 85 Km. This causes erroneous drift values[1] because the sudden simultaneous increase in amplitude at all antennas is interpreted as a very high speed. An example of the fading sequences and resulting cross correlations is shown in Figure 3.10. These particular data could be rejected on the basis of the N.T.D., which is 0.6 here.

3.3.3 Variant analyses for apparent velocity

Several methods were devised in an attempt to improve the data consistency. These were a least squares fit to time delays, a weighted least squares fit, a method of choosing peaks which gave the lowest N.T.D., and a method which required that the N.T.D. be zero.

The first two assume that the right peaks have been chosen, but that sampling or curve fitting errors may cause errors in the time delays. The solution for a least squares fit (working from equation 3.2) is:

$$\phi_a = \tan^{-1}\left(\frac{(t_{23}-t_{31})\sqrt{3}}{-2t_{12}+t_{23}+t_{31}}\right)$$

$$\frac{d}{V_a} = \frac{2}{3}\left[-t_{12}\cos\phi_a + t_{23}\cos(60^\circ-\phi_a) - t_{31}\cos(120^\circ-\phi_a)\right] \quad \ldots(3.3)$$

where V_a is the apparent pattern speed. This solution has been used by others (M.J. Burke, private communication) in a more complicated formulation designed for a non-equilateral antenna system.

1. see Appendix A, section A.3

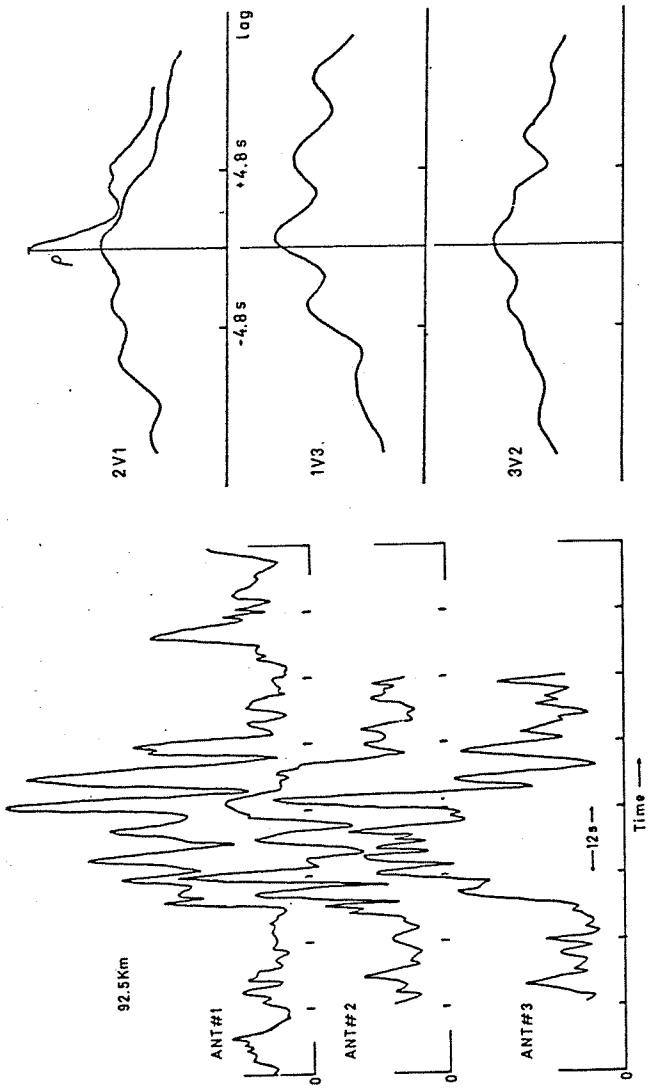

Figure 3.10 Example of (partial) fading sequence showing meteor trail echo, and the resulting cross correlations.

In the weighted least squares fit, the squared errors in times were weighted by the squared values of the maximum cross correlations. The equations are quite complicated unless a matrix formulation for a least squares fit is used (e.g. Hoel et al., 1971, Ch.4)[1]. The idea was that the greater peaks are more likely to be the correct ones, and should receive more weight. Of course, if the N.T.D. is zero, there is only one solution, and weighting has no effect on the results.

When these methods were put into practice, negligible improvement in the final wind consistency was found, and even to get similar quality, the same rejection criteria as before were needed. This was probably due to the fact that spurious peaks were still used.

Consequently, the methods requiring a low N.T.D. were tried. The method of lowest N.T.D. chose the two greatest peaks in each cross correlation, and then selected the combination of peaks giving the lowest N.T.D. A least squares fit to these delays produced a wind vector. The results were worse than the old analysis, apparently because there usually were a few spurious combinations with a low N.T.D.

The method of zero N.T.D. chose all combinations of lags in the cross correlation sequences defined by N.T.D.=0, and effectively constructed a contour plot of the sum of the cross correlation values versus two of the lag values (the third lag being determined by N.T.D.=0)[2]. The maximum value of the sum was found, and a paraboloid fitted to calculate the

1. see Appendix A, section A.1
2. see Appendix A, section A.4

exact delays for maximum sum. This variant gave about the same quality as the old analysis, probably due to the same reasons that lead to the failure of the 'method of lowest N.T.D.'.

The conclusions drawn from this exercise were that the peaks in the cross correlations had to be chosen very carefully before any further analysis was attempted.

3.3.4 Manual selection

By inspection of many cross correlation sequences from winter 1976 data, a rough set of criteria was devised for choosing peaks or rejecting data, and refined later into a systematic method. Essentially the requirements were that a chosen peak be about twice as large as any other peak in the sequence, and that the N.T.D. of the three time delays be < 0.2. This certainly rejected some 'good' data because two cross correlations might have only one significant peak and a secondary peak in the other (see Figure 3.9) might be the right one. However, since a large quantity of data was involved, these cases were rejected. The results (curve h in Figures 3.5 and 3.6) show spectacular improvement. Unfortunately there were little data left, and most of this was at low heights.

3.3.5 Reduced lag

In the course of examining the records, it was noted that there were only a negligible number of acceptable values (January to March) calculated from peaks with lags greater than 9 sec (i.e. speed $\geq$ 15 m/s). This suggested that, just by

choosing a smaller maximum lag, many of the spurious peaks could be avoided. This was done on data analysed by the old method by rejecting drift values with low speeds, and there is marked improvement as shown in Figures 3.5 to 3.8, curve g.

Of course, the lag should be large enough that good data will not be discarded. The choice of maximum lag is therefore a very difficult one, but it is felt that the improvement in quality makes up for any possible loss of data. Examination of April (summer) data indicated that a 12 sec maximum lag should be used. A method for determining the maximum required lag in each record will be discussed later.

These considerations certainly improved the wind values, but the N.T.D. distribution, even with a shorter maximum lag (curve c, Figure 3.4), is still much worse than that of other establishments.

3.3.6 Theoretical difficulties with apparent velocity

As discussed in section 3.3, the apparent velocity, V_a, only represents the true pattern velocity under the condition of an isometric pattern with no internal time change. This assumption cannot be tested with just the positions (lags) of the cross correlation peaks. If the pattern is very elongated, the apparent velocity will only determine the motion of the pattern perpendicular to its elongation (Phillips and Spencer, 1955, show the relations between these parameters) giving speeds which are too low, and a wrong drift direction. In addition, time change in the pattern as it moves will distort

the cross correlation peaks towards zero lag. The latter can be illustrated by imagining a one dimensional pattern moving between two antennas as in Figure 3.11. If there is no time change in the pattern, then the cross correlation should be unity at some lag which depends on the speed. If there is time change, then the time component of the cross correlation should decrease with increasing lag. The resultant peak is thus shifted towards zero lag, and so the apparent velocity is greater than the 'true' velocity.

3.4 Full correlation analysis

A method which corrects for time change has been developed by Briggs et al.(1950), and extended to non-isometric patterns by Phillips and Spencer (1955). The resulting drift vector is called the 'true' velocity, V. The method is called Full correlation analysis (FCA) because it makes use of the full cross correlation peaks, not just the time lags for maximum correlation. Variant methods also exist, e.g. the 'straight line method' described by Briggs et al.(op.cit.), and the least squares fit of Fedor (1967).

The initial papers are rather difficult to understand, so the derivation of relevant equations here will roughly follow the very concise formulation of Fedor.

3.4.1 Derivation of relevant equations

The spatial-temporal correlation function seen by an observer moving with the average drift of the pattern will

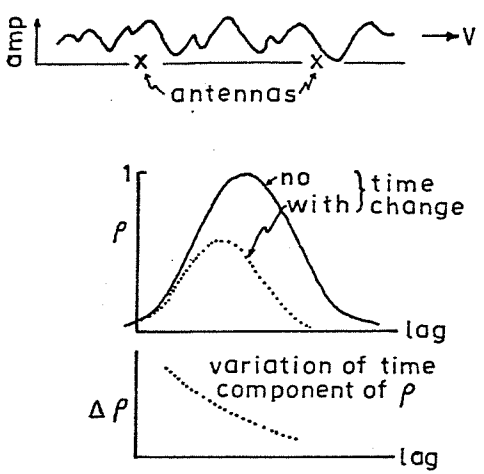

Figure 3.11 Illustration of the increase in apparent velocity when the pattern has internal time change.

be represented by:

$$\rho(x,y,t) = F\left(\frac{x^2}{a^2} + \frac{y^2}{b^2} + \frac{t^2}{c^2}\right) \qquad \ldots(3.4)$$

where x and y are measured along the average axes of symmetry in the pattern, F is a monotonically decreasing function which has the value 1 at zero argument, a and b are a measure of the pattern scales along the axes, and c is a measure of the internal pattern time change. Thus, if the observer measures the spatial pattern at some instant and shifts it by the vector distance (x,y), the spatial correlation between this shifted pattern and the unshifted will be $\rho(x,y,0)$; here the time difference is zero because both patterns refer to the same instant in time. If he then correlates pairs of amplitudes with a fixed delay, t, at his location (i.e. zero spatial shift), the result will be $\rho(0,0,t)$. From equation 3.4, it can be seen that surfaces of constant correlation are ellipsoidal in x,y,t space.

When measurements are being made from a fixed reference system, the effect on the observed correlation function is as if the observer were moving 'backwards' at velocity V (the drift velocity of the pattern), and he will see a correlation function:

$$\rho(x',y',t) = F\left(\frac{(x'-V\cos\phi't)^2}{a^2} + \frac{(y'-V\sin\phi't)^2}{b^2} + \frac{t^2}{c^2}\right) \qquad \ldots(3.5)$$

where x' and y' are coordinates in the fixed system, illustrated

in Figure 3.12. Transforming to geographic coordinates, (r,s), by:

$$x' = r\cos\theta + s\sin\theta$$

$$y' = -r\sin\theta + s\cos\theta,$$

gives the correlation function:

$$\rho(r,s,t) = F\left(\frac{(r\cos\theta + s\sin\theta - V\cos\phi' t)^2}{a^2} + \frac{(-r\sin\theta + s\cos\theta - V\sin\phi' t)^2}{b^2} + \frac{t^2}{c^2} \right) \quad \ldots(3.6)$$

This last expression gives the value of correlation between amplitudes at a pair of ground locations with orientation and spacing according to the vector (r,s), which are compared with a delay of t.

Two basic assumptions have been made in this derivation. Firstly, ignoring time changes, contours of constant spatial correlation are assumed to be ellipses, the major axis being the direction of preferred elongation in the pattern. This is reasonable, provided the argument of F is not too large, since it is a first approximation to the variation near the maximum of any well behaved function (Briggs et al.,1950). Secondly, time variations are assumed to follow the same statistics (within a scale factor) as spatial variations, and are independent of them. Briggs (1968) has described a method for calculating the drift velocity without the latter assumption.

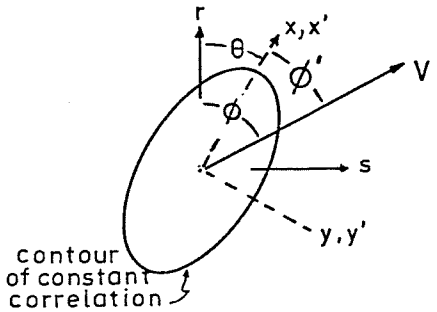

Figure 3.12

Definition of coordinate system and parameters used in the development of full correlation analysis.

Figure 3.13

Choice of antenna pair vectors forming closed path.

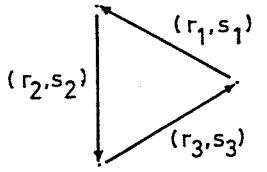

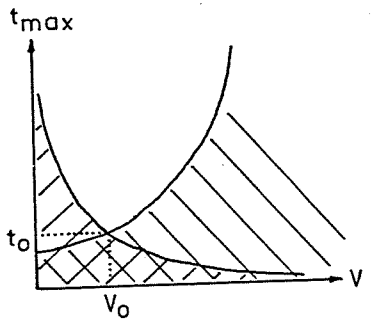

Figure 3.14

Illustration of choice of maximum required lag. Lag must be in both shaded areas simultaneously

3.4.2 Analysis methods

The most common methods for analysing the data to find the pattern and drift parameters involve a comparison of time lags for equal correlations, thus avoiding a definition of the correlation function F. For example, for a pair of antennas defined by (r_i,s_i), the lag, t_i, for which the auto correlation (assumed the same at all antennas) is equal to the cross correlation at zero lag produces the three equations

$$\rho(0,0,t_i) = \rho(r_i,s_i,0) \; ; \; i=1,2,3 \; ,$$

where a non-collinear arrangement of three antennas is used. Also, the lag, t_i', for which the auto and cross correlations are equal gives the three equations

$$\rho(r_i,s_i,t_i') = \rho(0,0,t_i') \quad ; \; i=1,2,3 \; ,$$

and the value of lag, t_i'', for which the auto correlation equals the maximum value of cross correlation (for which the lag, t_{max_i}, is known) gives the three equations

$$\rho(r_i,s_i,t_{max_i}) = \rho(0,0,t_i'') \; ; \; i=1,2,3 \quad .$$

By selecting suitable combinations of these nine equations, exact calculation of five parameters (generally V, ϕ', θ, a/c, b/c) can be made. When the pattern is assumed isometric then a=b, and a/c is denoted V_c.

In order to get absolute pattern scales, which may be compared from record to record, an absolute measurement of correlation is required. Briggs (1967, U. of Adelaide report) uses the value of lag for which the auto correlation is 0.5.

As seen in Figure 3.9, there are cases in which this type of analysis will fail or give spurious drift values either

because some cross correlations are negative at zero lag, or because of their skewed nature.

3.4.3 Straight line method

A more advanced method, called the 'straight line method' was described by Briggs et al. (1950) and modified by Keneshea et al. (1965). A plot of $t_a^2 - t_{c_i}^2$ versus t_{c_i}, where t_a and t_{c_i} are lags for which the auto and i^{th} cross correlation have equal values, should be a straight line. The equation of the line is obtained by setting $\rho(r_i,s_i,t_c)$ equal to $\rho(0,0,t_a)$, and is found to be:

$$(t_a^2-t_c^2)\left[\frac{V^2\cos^2\phi'}{a^2} + \frac{V^2\sin^2\phi'}{b^2} + \frac{1}{c^2}\right] = \left(\frac{(r_i\cos\theta + s_i\sin\theta)^2}{a^2} + \frac{(-r_i\sin\theta + s_i\cos\theta)^2}{b^2}\right) + t_c\left[\frac{-2V\cos\phi'}{a^2}(r_i\cos\theta + s_i\sin\theta) + \frac{-2V\sin\phi'}{b^2}(-r_i\sin\theta + s_i\cos\theta)\right] \qquad \ldots(3.7)$$

Although it is not obvious from the above, the three straight lines only yield five parameters as before. This is because the slopes of the lines must satisfy another equation equivalent to N.T.D. = 0. Proof of the latter will follow shortly. In order to get absolute pattern scales, the (unrealistic) functional form $\rho(0,0,t) = 1-(Bt^2)^n$ was assumed, and two points from the auto correlation were used to solve for B and n.

This is a good method in that it demonstrates the applicability of the assumptions for full correlation analysis and the straight line fit avoids dependence on single values of correlation. However, for routine processing, the advantage is lost because of the time involved in examining the plots. Also much of our data is not suitable for this analysis.

3.4.4 Proof that N.T.D. = 0

It is useful at this point to show that the N.T.D. is theoretically zero under these more general conditions, because it is a very powerful parameter for preselection of data. N.T.D. $= \left| (\sum t_{max_i}) / (\sum \left| t_{max_i} \right|) \right|$ where the set of times is from the cross correlations for antenna pairs (r_i, s_i) taken around a closed path (see Figure 3.13). It is sufficient to show that $\sum t_{max_i} = 0$.

Differentiation of equation 3.6 to find the lags for maximum cross correlation gives:

$$t_{max_i} = \frac{\frac{V\cos\phi'}{a^2}(r_i\cos\theta + s_i\sin\theta) + \frac{V\sin\phi'}{b^2}(-r_i\sin\theta + s_i\cos\theta)}{\frac{V^2\cos^2\phi'}{a^2} + \frac{V^2\sin^2\phi'}{b^2} + \frac{1}{c^2}} \qquad \ldots(3.8)$$

Since V, ϕ', a, b, and c are assumed constant, this equation reduces to

$$t_{max_i} = \alpha r_i + \beta s_i ,$$

where α, and β are constants. But since a closed path is involved, $\sum r_i = \sum s_i = 0$, and so the N.T.D. =0. Comparison

of equations 3.7 and 3.8 shows that the slope of the i^{th} straight line is $-2t_{max_i}$, so that the sum of the slopes must be zero.

The spaced receiver, spaced frequency method (Fedor,1967) is presently being used to determine vertical motions (Wright et al.,1976; Misra,1974) and it is of interest to inquire whether the N.T.D. = 0 in cases when these are important. The correlation function seen by a fixed observer in this case (Fedor,1967) is

$$\rho(x,y,z,t) = F\left(\frac{(x-V_x t)^2}{d_x^2} + \frac{(y-V_y t)^2}{d_y^2} + \frac{(z-V_z t)^2}{d_z^2} + \frac{t^2}{c^2} \right) \qquad \ldots(3.9)$$

where the axes of symmetry in the pattern are retained for simplicity; d_x, d_y, and d_z are pattern scales, the vertical difference in sample height, z, is created by a small change in transmitted frequency (only total reflection, e.g. E region, echoes can be used) and V_x, V_y, and V_z are the drift components along the axes. By differentiating as before, t_{max_i} is found to be $\alpha x_i + \beta y_i + \gamma z_i$ where α, β, and γ are constants. When amplitudes are sampled in the horizontal plane, z_i is zero; and the first two terms cancel when summed around a closed path. Thus the N.T.D. is also zero here.

3.4.5 Chosen analysis method

The problem with the preceeding methods (e.g. sections 3.4.2 and 3.4.3) on U of S data is that they are basically graphical, viz. examination of the cross correlations or

assumption of good data is necessary. In the case of single point methods (section 3.4.2), too much dependence is placed on the fitting of curves to local segments to find a particular value. Given U of S data with sometimes skewed cross correlations, and generally low values (quite often negative at zero lag) these are hopeless. This was demonstrated by the use of an existing FCA graphical analysis method (D.T. Rees, private communication) which produced data of poor quality and quantity, no better than the apparent velocity analysis described in section 3.3.1.

Fedor's (1967) solution which identified the correlation function F with a Gaussian, and made a least squares fit to the data was finally chosen. This is a particularly good method for automatic analysis because the parameters are over-determined (i.e. a few bad values can be tolerated). The correlation function is now:

$$\rho(r_1,s_1,t) = \exp\left[-\tfrac{1}{2}\left(\frac{(r_1\cos\theta + s_1\sin\theta - V\cos\phi' t)^2}{a^2} + \frac{(-r_1\sin\theta + s_1\cos\theta - V\sin\phi' t)^2}{b^2} + \frac{t^2}{c^2}\right)\right] \qquad ...(3.10)$$

and a least squares fit of this function to the experimental auto and cross correlation sequences gives the six FCA parameters directly. The pattern scale parameters a, and b, and time change parameter c (called the characteristic time) refer to a correlation value of 0.61 (i.e. $e^{-\frac{1}{2}}$). The drift direction is given by $\phi = \phi' + \theta$. The tilt angle of the

major axis (0-180°) defines pattern orientation. The standard practice is to measure all angles East from geographic North. A detailed description of the data selection criteria and analysis is given in Appendix C.

3.4.6 Further comments

It is interesting to note that the Gaussian assumption requires that all correlations (auto and cross) be Gaussian in shape and have equal width (in lag). This can be shown as follows.

$$\rho(t) = \exp\left[-\tfrac{1}{2}\ (ut^2+vt+w)\right]$$

is the general form of the correlation function where u,v, and w are constant for a given pair of antennas. This can be re-written as:

$$\rho(t) = \exp\left[-\tfrac{1}{2}\ u\left[(t+\tfrac{v}{2u})^2 + (\tfrac{w}{u} - \tfrac{v^2}{4u^2})\right]\right]$$

where u depends only on the drift and pattern parameters, not on the orientation or spacing of the antenna pair. The first term gives the variation with lag and is seen to be Gaussian with 'width' 1/u. The second term is just a constant scale factor. Thus, for example, the widths (in lag) of all the correlation peaks measured at half their maximum value are equal.

This suggests that all the correlations, and thus the drift and pattern parameters can be defined with just the width of the auto correlation, and the positions and magnitudes of the maxima in the cross correlations. These parameters

happened to be available on previous computer output for other reasons, and so a "Poor Man's" full correlation analysis was developed to reprocess this data, and is derived in Appendix D.

3.4.7 Variable lag limits

Now that rules have been laid down for determining pattern scale, time change, and true velocity, the question of setting a maximum lag, beyond which no significant cross correlation peaks should occur, may be considered. If a usable limit can be found, this would constitute an important improvement because it would remove a few more spurious peaks from consideration. Since the calculation of cross correlations is the most expensive part of the analysis, a solution would be of economic interest as well.

The problem will be approached from the point of view that only peaks of reasonable size are sought in the cross correlations. Very small peaks could easily be due to random sampling effects and are of no interest.

Two factors operate to reduce the magnitude of the peaks; one is pattern scale (in combination with antenna separation) and the other is time change in the pattern. The position of a peak in lag is determined by the apparent velocity (i.e. the velocity found from t_{max_1}). It turns out that, due to internal time change and the predominance of pattern elongations perpendicular to the drift, apparent velocity is almost always

greater than the true velocity V (see Figure 3.18). Thus if V is used to estimate the maximum lag at which a peak will occur, it will over estimate.

Two inequalities will be developed which must simultaneously be satisfied in order that the peaks be significant ($\rho > 0.13$ is convenient here, although any limit could be used). Firstly assume an isometric pattern of scale a, and consider that pair of antennas whose direction lies closest to the drift direction. The peak for this pair will have the greatest lag. Then, for this one dimensional situation, the auto correlation is given from equation 3.5 by:

$$\rho(0,t) = \exp\left[-\tfrac{1}{2}\left(\frac{(0-Vt)^2}{a^2} + \frac{t^2}{c^2}\right)\right] \quad ,$$

and the cross correlation by:

$$\rho(d,t) = \exp\left[-\tfrac{1}{2}\left(\frac{(d-Vt)^2}{a^2} + \frac{t^2}{c^2}\right)\right] \quad ,$$

where d is the antenna separation. The cross correlation at zero lag, an estimate of pattern scale, is:

$$\rho_o = \exp\left[-\tfrac{1}{2}\frac{d^2}{a^2}\right] \qquad \ldots(3.11)$$

and the auto correlation at any lag T is:

$$\rho_T = \exp\left[-\tfrac{1}{2}\left(\frac{(VT)^2}{a^2} + \frac{T^2}{c^2}\right)\right] \qquad \ldots(3.12)$$

The latter equation may be used to estimate the time change parameter, c :

$$c = \sqrt{\frac{1}{\frac{-2\ln\rho_T}{T^2} - \frac{V^2}{a^2}}} \qquad \ldots(3.13)$$

This parameter is important because, just due to time change in the pattern, any value of ρ must be less than 0.13

(i.e. e^{-2}) at a lag $t > 2c$. Since peaks with $\rho < 0.13$ are of no interest, the first inequality is:

$$\ell_{max} \leq 2c = \sqrt{\frac{2}{\frac{-2\ln \rho_T}{T^2} - \frac{V^2}{a^2}}} \qquad \ldots(3.14)$$

where ℓ_{max} is the maximum lag over which it is necessary to search for peaks. Substitution of the pattern scale, a, from equation 3.11 into equation 3.14 gives:

$$\ell_{max} \leq \sqrt{\frac{2}{\frac{-2\ln \rho_T}{T^2} + \frac{V^2}{d^2} 2\ln \rho_o}} \qquad \ldots(3.15)$$

For the second inequality, recall that $t_{max} = d/V_a$ for the one dimensional case, and $t_{max} \leq d/V_a$ for the two dimensional case. Since it has been assumed that $V \leq V_a$, then:

$$\ell_{max} = t_{max} \leq \frac{d}{V} \qquad \ldots(3.16)$$

The only unknown in these two inequalities is V. Figure 3.14 shows the right hand sides of equations 3.15 and 3.16 as a function of V. Both curves are monotonic, so that ℓ_{max} only satisfies both inequalities when it is below the intersection point, (t_o, V_o), which is given by:

$$\frac{d}{V_o} = \sqrt{\frac{2}{\frac{-2\ln \rho_T}{T^2} + \frac{V_o^2}{d^2} 2\ln \rho_o}}$$

$$t_o = T\sqrt{\frac{\ln \rho_o - 2}{\ln \rho_T}} \qquad \ldots(3.17)$$

Thus the required limit is:

$$\ell_{max} = T\sqrt{\frac{\ln \rho_o - 2}{\ln \rho_T}} \qquad \ldots(3.18)$$

Returning to two dimensions, there are three values of ρ_o, and it is reasonable to choose the one which gives the largest limit (i.e. the smallest value of cross correlation at zero lag), although in very special cases this may slightly underestimate the lag limit. For data in which this value is negative, one must revert to the maximum lag considered reasonable for the season, as discussed previously. In practice, the values (T, ρ_T) are taken from one point on the auto correlation (at $\rho \approx 0.5$), and a 'safety margin' of about 20% is added to the calculated lag limit, ℓ_{max}.

Examination of experimental data has not indicated a single case where this limited lag excludes a 'good' peak in the cross correlations.

3.5 Results of FCA method

The consistency of wind values from this FCA method as applied to U of S data is shown in Figure 3.5 to 3.8 (curve c), and a major improvement is seen. It is felt that most of this is due to the preliminary rejection of data with N.T.D. ≥ 0.3, and better selection of peaks, rather than the use of FCA. This does not mean that V_a is as accurate as V, because pattern scales, orientation, and internal time change may vary over longer periods of time and greater height separations than those used to determine consistency. These variations would perturb V_a, but not V.

Since pattern scales were available from the FCA , these were compared with the antenna spacing to see whether this

factor could explain our low values of cross correlation. Analysis on the existing equilateral antenna system (270 m spacing) yielded, on records that could be processed, patterns of median minor axis 120 m, and median major axis 190 m. This means, for example, that the cross correlation at zero lag for an antenna pair aligned in the direction of the minor axis would be about 0.1 on the average. This can explain, at least, the negative values at zero lag; and also partially explains the low values of maxima, although the latter are also dependent on other factors, e.g. pattern speed and direction.

3.6 Reduced antenna spacing

In an attempt to raise the 'correct' peaks above the spurious ones, smaller antenna spacing was proposed. The easiest way to accomplish this was to erect an antenna in the centre of the present equilateral triangle. This arrangement could be used to simulate a small equilateral triangle by using pairs of antennas consisting of the centre and one of the originals, and reduced the spacing to 156 m (a factor of approximately 2).

Since fading at all four antennas is recorded, both sizes of triangle are available for separate analysis. There has been some evidence (Golley and Rossiter,1970) that the calculated true velocity depends on antenna spacing. This could be due to the breakdown of the ellipsoid assumption at large arguments of the correlation function F, or to the effects of coupling between antennas (Fedor and Plywaski,

1972). Observations indicated that the calculated velocity is smaller for closer spacing.

In order to check whether such a bias exists at our location, a set of data was analysed for both triangle sizes, and the subset of records for which both calculations were possible (according to the criteria in Appendix C) was extracted. Unfortunately, the large triangle values were of much poorer quality here than when the large triangle alone is used. The reason for this is not known as yet, but differences in sampling rate and amount of raw data averaging may be responsible[1] The isolation between centre and outer antennas was measured as ~50 dB, and the coupling between the original antennas did not increase noticeably when the centre antenna was erected, so this is probably not the cause. Figure 3.15 compares the parameters produced by both antenna spacings. The velocity is seen to be unbiased, based on medians, but the pattern scale is larger for the large triangle. The consistency of the small triangle wind values is shown in Figures 3.5 to 3.8 (curve d) and the N.T.D. distribution in Figure 3.4 (curve d).

The percentages of output available from small and large (when recorded alone) triangles are compared in Table 3.2. These are calculated with respect to the number of records which passed the preliminary criteria of standard deviation and fading rate as explained in Appendix C. The data sets analysed are different, of course, but it appears that the use of the smaller spacing has almost doubled the amount of

1. see Appendix B

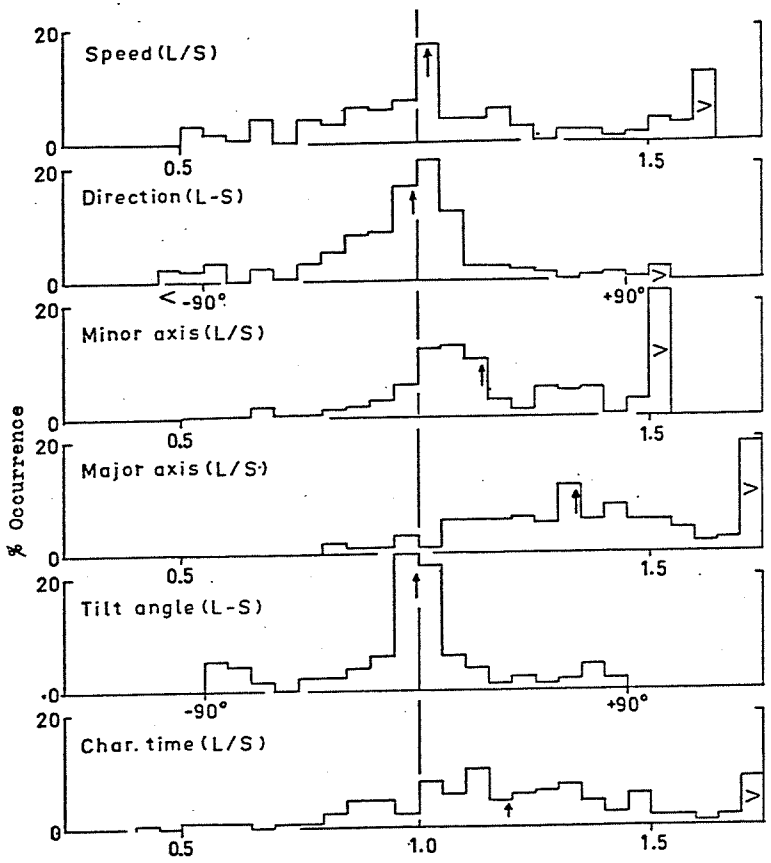

Figure 3.15 Comparison of FCA parameters for large and small antenna spacing. Median values are shown by arrows.

Table 3.2 Percentages of data available

configuration and height range		Percentage
small triangle:	52-82 Km	86
	85-103 Km	50
	106-118 Km	51
	all heights	58
large triangle:	all heights	30

output.

It is interesting to note that the N.T.D. distributions are very similar (curves c and d, Figure 3.4), the small triangle giving only a small improvement. One point not mentioned previously is that the N.T.D. is only calculated for records in which a local peak (≥ 0.1) is found in each cross correlation, and the percentages in Figure 3.4 are with respect to the number of these. The latter number, as a percentage of the number of records passing the preliminary rejection criteria, is 77% for the large, and 95% for the small triangle. Thus the small triangle apparently did not improve the consistency of the data, as illustrated by curves c and d in Figures 3.5 to 3.8 (although different data sets are being compared), but made more of it available just because correlation peaks which were too small to see with large antenna spacing became significant with small.

This result seems to contradict the theory that poor wind values were the result of spurious peaks being taken for the correct ones, because if the spurious peaks remained the same size when the spacing was decreased, then the right peaks (i.e. low N.T.D.) should have been chosen more often.

The conclusion must be that the poorer quality of our data is due to ionospheric conditions, and this is probably connected with the oblique echoes problem in the DAE. Examination of winter 1976 data revealed that the best quality wind data were obtained on a day when there was no evidence of oblique echoes in the DAE.

It is noted as well that the quality of data, according to the N.T.D. distribution, has an important variation with height, as shown in Figure 3.16, being best at lower heights. Thus the availability of echoes at various heights may create apparent differences in quality between different data sets, or different locations.

3.7 Comparison between apparent and true velocity

Since both apparent and true velocities will be used in the following work, it is useful to compare their values for long term averages. The two factors which contribute to differences between V_a and V are pattern tilt angle (with respect to drift direction) and internal time change. The first causes a difference in computed direction and makes $V_a < V$ (e.g. Phillips and Spencer,1955), as noted in section 3.3.6. Thus it is possible that $V_a < V$ if the tilt is not perpendicular (or parallel) to the drift and internal time change is negligible.

Generally time change is not negligible, and so $V_a > V$ (see section 3.3.6). This is especially true when a meteor trail occurs during a record. Here the velocity produced by FCA is usually, except in very special circumstances, reasonable[1] (e.g. < 100 m/s), whereas the apparent velocity can be several hundreds of metres per second. The question of whether FCA determines the correct velocity, and it does seem to, in these situations must be left to future work.

Distributions of tilt angle, relative to drift direction, are shown in Figure 3.17. About 40% of the data is within

1. see Appendix A, section A.3

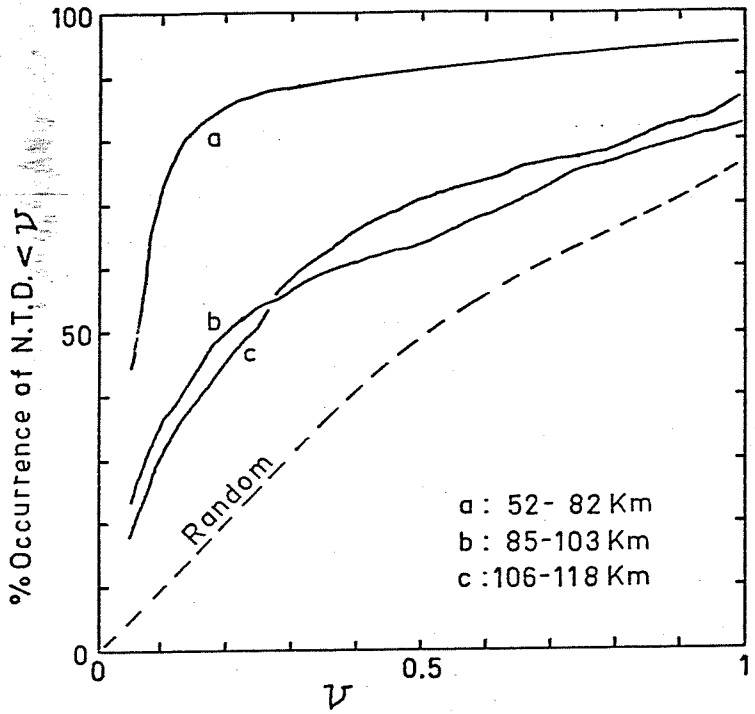

Figure 3.16 Variation of N.T.D. distribution with height (small triangle, day).

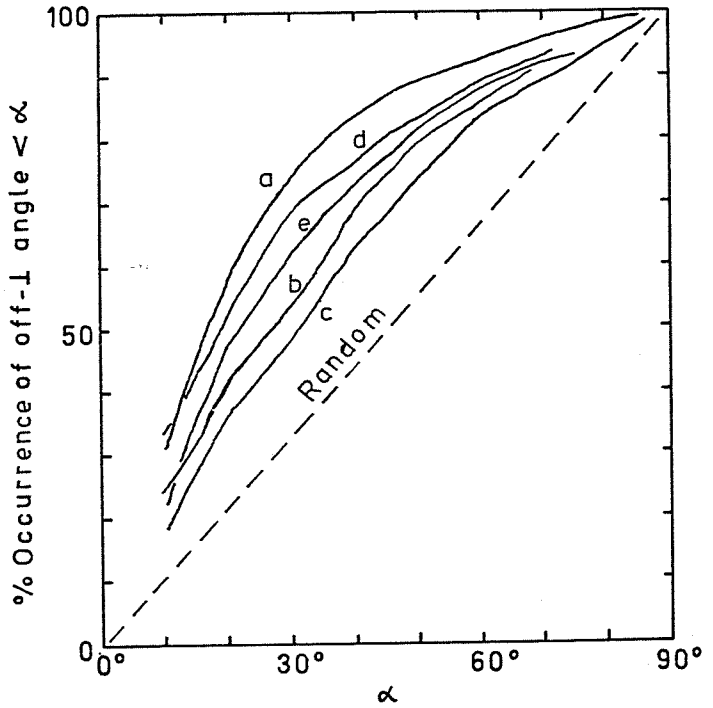

Figure 3.17 Distribution of off-⊥ angle of major axis of pattern with respect to drift angle. Small triangle; a:52-85 Km, b: 85-103 Km, c:103-118 Km (winter, noon). Large triangle; d: all hts.(winter, day), e: all hts.(summer,noon).

20° of perpendicular, so it can be generally assumed that apparent and true directions agree. This is a rather strange result, that the pattern is linked in some way to the drift velocity, and more will be said on this matter.

Histograms of the ratio of apparent to true speed and direction differences are shown in Figure 3.18. For the lowest height range $V_a \simeq V$, but at higher heights, where meteor trails may occur, the ratio can be large.

Figure 3.19 compares a five hour average of data processed by the old analysis (V_a, section 3.3.1) and by the new FCA (V). It can be seen that below ~100 Km the magnitudes are comparable, partly because the scatter in the old analysis values reduces the mean. Above this height $V_a \simeq 2V$.

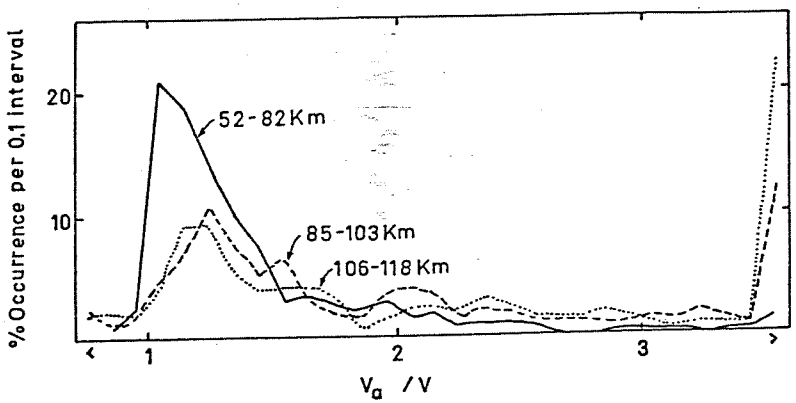

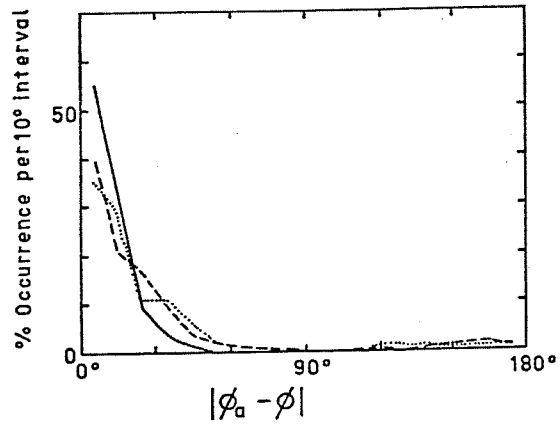

Figure 3.18 Comparison of apparent and true velocity, speed and direction.

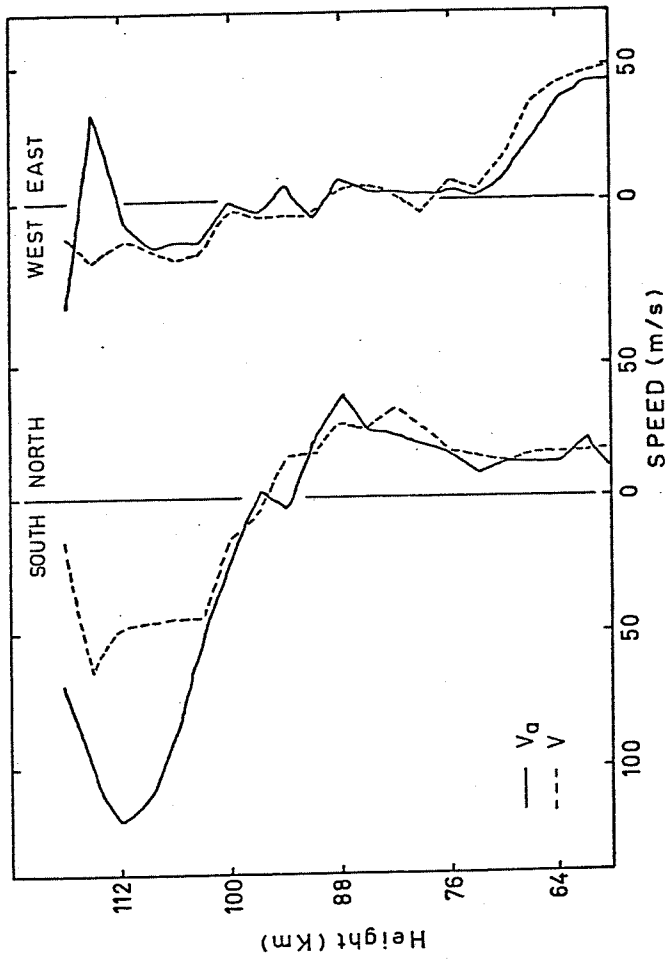

Figure 3.19 Comparison of apparent (old analysis) and true velocity in averages(5 hr).

CHAPTER IV

INTERESTING WINDS RECORDS

4.1 Introduction

The following discussion will be based solely on the appearence of the cross correlations, since it is quite feasible to print these out in compressed form with each fading record analysis. The records shown are not intended to be representative (but are not entirely unrepresentative either); in fact, most would not have led to a wind calculation according to the present criteria. However, it is possible to retrieve some of the rejected data by examination of the cross correlations if continuity of wind data is considered important. Five records are discussed.

4.2 Large NTD in an otherwise acceptable record.

Figure 4.1 shows a case in which the correlation peaks are relatively large and unique, but the NTD $\sim$0.6. Only a partial plot has been shown from the maximum calculated lag of $\pm$ 21 ($\pm$ 12 sec), but there was only one other peak, of magnitude 0.15, in ρ_{32} at + 19 lags. If the symmetrically shaped peaks are taken to be correct, then NTD=0 predicts a peak in ρ_{32} at the arrowed position. One can imagine a peak here which is overlapped by a 'spurious' larger peak centred at +1 lag. A comparison of the widths (at half amplitude) of the mean auto correlation, ρ_{21}, and ρ_{13} suggests that these widths are equal for this pattern motion. If the fading is such that the

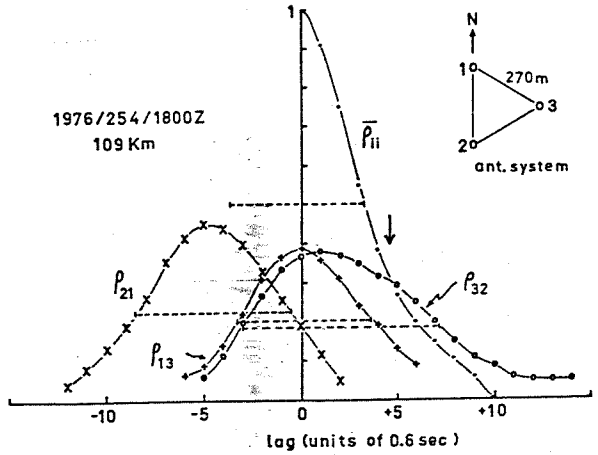

Figure 4.1 Record showing well defined cross correlation peaks but large NTD (~0.6). Half-widths of auto and cross correlation peaks are shown as dashed lines. The arrow indicates the expected position of the peak in ρ_{32}.

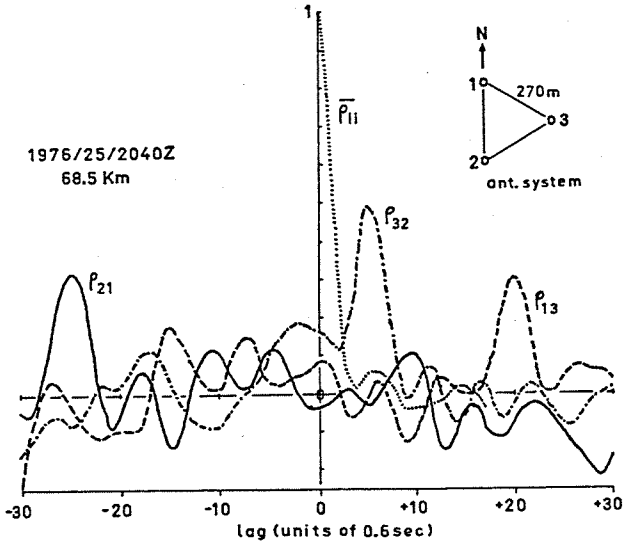

Figure 4.2 Record with well defined peaks at large lags, indicating very low speed and little internal pattern time change.

correlation function F (see section 3.4.1) is Gaussian, then this is a necessary result (see section 3.4.6). One can also imagine a similar width for the 'concealed' correct peak in ρ_{32} by measuring the width from the expected peak position towards +ve lag at a correlation value of ~ 0.15 (which is approximately half the concealed peak value). Thus, by careful examination of this record, enough information can be gleaned to calculate a wind value. The point of interest is the existance of the large 'spurious' peak, however. What would cause such a peak ? It is presumably not due to a small change in wind during recording, otherwise the other peaks would also be skewed, or even double (although the 'correct' wind change could cause this record). If it is due to a second, superimposed, pattern motion, then there should be two other peaks in the other two cross correlations with lags defined by NTD=0 (i.e. $t_{21}+t_{13}+1=0$). If these were small, they could be hidden by the primary peaks, but the related pattern parameters would probably have to be quite different from the 'major' pattern motion. If the speed of this second pattern motion were very low ($\lesssim$ 10 m/s), they could be located outside maximum lag.

The postulation of a second pattern motion raises another question. Are the peaks arising from each motion reduced in magnitude due to the existance of the other? Appendix E attempts an answer to this question, and shows that serious modification to velocity values may occur in such cases.

4.3 Large delay times.

Figure 4.2 shows correlations for a case in which there are relatively few spurious peaks, and the correct peaks (NTD ∽ 0.1) are at very great delays. Analysis gave axes of 238 and 14 m, a tilt angle almost exactly perpendicular to the drift direction, and V_a, $V \sim 8$ m/s, $\tau_0 \sim 10$ sec. The fading sequences have not been examined, but it appears that these data result from the passage of a single long, thin, pattern feature. The auto and cross correlations do not indicate a cyclic wave pattern, such as will be shown in the next section. It should be noted that in such extreme cases (i.e. large axial ratio) the parameters have been found to be quite sensitive to small changes in analysis method.

4.4 Interference fading.

Figure 4.3 shows a record in which interference fading is quite obvious. Strong echoes from a few scatterers interfere to cause a wave-like pattern on the ground. Interference between X and O modes might also cause this effect. There must also be a fairly strong low frequency component in the fading, since all the correlations are positive over the calculated lag. There are many possible choices of peaks for NTD∽0. Three are shown. The set marked ↕ might be chosen for analysis under the 'doubtful data' category (see section C.4d) if the peak at -3.5 lags in ρ_{21} were larger than that at -0.5 lags. The high and low frequency components seem to have similar delays in each cross correlation. A possible interpretation

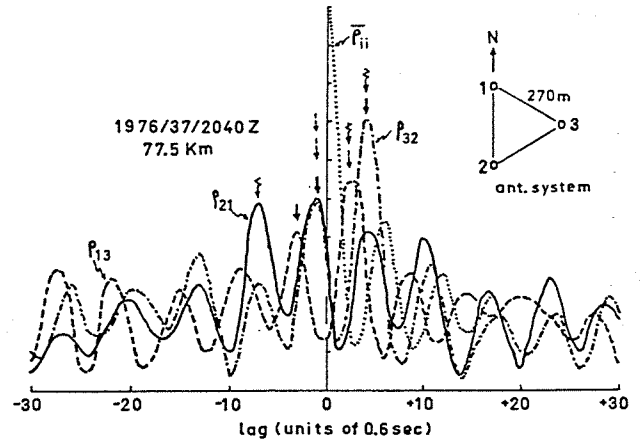

Figure 4.3 Record showing wave pattern, probably caused by interference between echoes. Several sets of peaks with low NTD are arrowed.

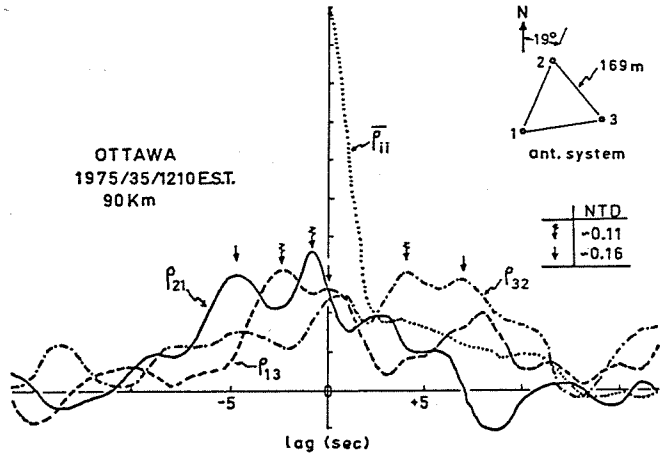

Figure 4.4 Illustration of double peaks in cross correlations, probably caused by sampling over a shear in wind.

of these data is that the low frequency component represents the passage of relatively large irregularities and the high frequency represents interference between the echoes from each. If the scatterers were not moving relative to each other, both patterns would have the same apparent velocity (i.e. t_{max_1}).

4.5 Double peaked correlations.

Figure 4.4 shows a record from Ottawa in which the sample range (~7.5 Km) either covers a shear in wind with height, or an abrupt change in wind occurs during the record. The two arrowed sets of peaks each have relatively low NTD. Appendix E discusses the effect of simultaneous pattern motions on the calculated velocity. By making a few simplifying assumptions, it is shown that the peak correlation values will be reduced, which in turn will lead to low velocity values. If a least squares fit to a Gaussian is employed (sight unseen), the resulting fitted correlations will be too wide for either pattern motion. The latter also leads to low velocities (see Appendix E). Thus, probably the best method to use is the Poor man's FCA (Appendix D), although the calculated velocity will still be biased. This type of record is seldom seen in our data, probably because of our smaller sample range (~3 Km).

4.6 Very low cross correlation peak.

Figure 4.5 shows a case, recorded with small antenna spacing, in which a peak in one cross correlation is very low. It appears to be a correct peak, because the large peaks in the

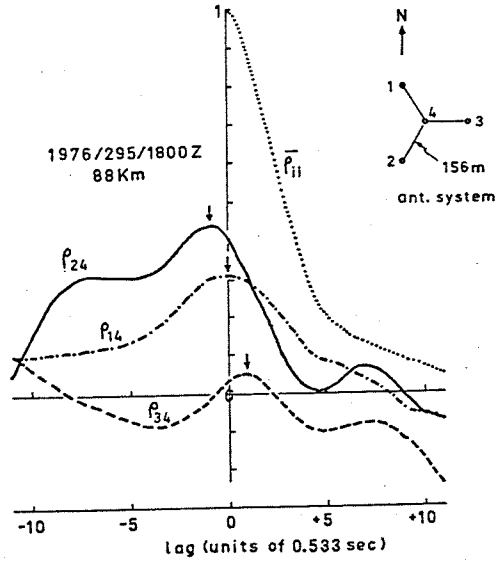

Figure 4.5 Record in which two cross correlation peaks are relatively large, but the third is near zero.

other cross correlations predict this position from NTD=0. This record would not normally be analysed because there are no local peaks in ρ_{34} greater than 0.1. A fairly large 'spurious' peak is also seen in ρ_{24} at -5 lags, and a strong low frequency component is evident in ρ_{34}, so that analysis would produce doubtful results in any case. It is likely that removal of the low frequency perturbation would make analysis worthwhile.

CHAPTER V

PATTERN PARAMETERS

5.1 Introduction

Four sets of data are discussed; two intensive ten runs in August and October 1976 from Sasaktoon, two noon hours (Feb 4,7, 1975) from Ottawa (Communications Research Centre), and three hours of Adelaide data (Feb 18,1976) taken near noon. A much more extensive analysis of Adelaide data has been done by Stubbs (1977). Since two of the parameters (pattern scale and characteristic time) have been found to depend fairly strongly on equipment (antenna spacing) and analysis parameters, cross comparisons between different data sets are difficult. Table 3.1 has shown equipment parameters for Ottawa and Adelaide data. The effect of the transmitter antenna beamwidth is not considered, but is liable to be an important parameter when comparing data from different research establishments.

Three equipment configurations have been used at U of S, as we are in the process of modifying both the antenna system and analysis. The August ten day run employed the large triangle system (see Figure 1.1) before the centre antenna was erected. The October data were recorded on all four antennas, permitting analysis for both large and small spacing, but the resulting quality of wind values from the large triangle was found to be much poorer than when the former configuration (August) was used. The reason for this is still unclear, but it is possible that the pattern parameters are affected as well.

It is convenient to represent the pattern scales and char-

acteristic time by the ρ=0.61 (i.e. $e^{-\frac{1}{2}}$) correlation values. Thus, values from other analyses using ρ=0.5 (e.g. Briggs et al., 1950) must be divided by 1.18 (based on the assumption of Gaussian correlations) before comparison. The parameters to be compared are $\sqrt{AB}$, where A and B are the major and minor axes respectively of the correlation ellipse; the characteristic time τ_c (also denoted C), which defines the internal time variation in the pattern; A/B, the axial ratio; the characteristic velocity in the direction of drift, V_{c_V}, defined in Figure 5.1; and the amount by which the tilt angle of the major axis is off-$\perp$ with respect to the drift direction. It is not clear how the Adelaide parameter is defined, since this strictly only applies to isometric patterns; however, axial ratios at Adelaide are relatively low, so that the direction in which V_c is taken is not very important. This will lead to a small bias in U of S and Ottawa values, since elongation is usually nearly perpendicular to the drift, which will make V_{c_V} smaller than the 'average' value of V_c.

5.2 Comparison of parameters.

Figure 5.2 shows results from the August 1976 ten day run (Saskatoon). The plotted values were obtained as follows. Firstly, the medians were calculated at each recorded height over each hour (there was a maximum of 12 determinations per hour), except for V_{c_V}, for which RMS values were used. Then the medians of these hourly values were calculated for day (12-23Z) and night (0-11Z). A separate calculation had weighted each

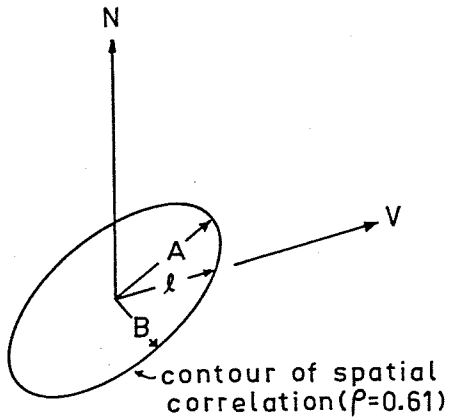

$$V_{cV} = \frac{l}{\tau_c}$$

Figure 5.1 Definition of V_{c_V}

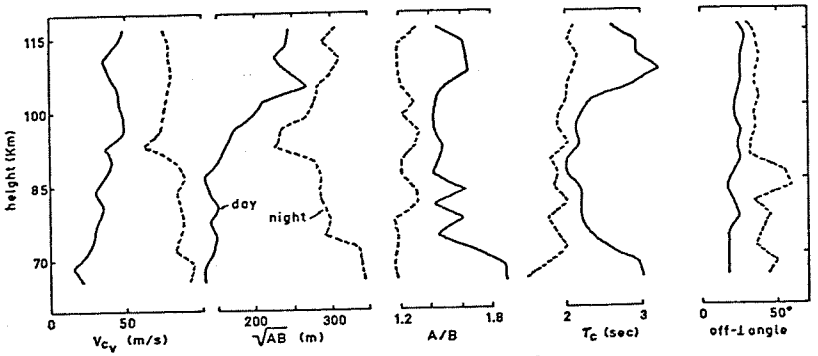

Figure 5.2 Median pattern parameters (ρ=0.61) for August 1976 (Saskatoon), large triangle (270 m).

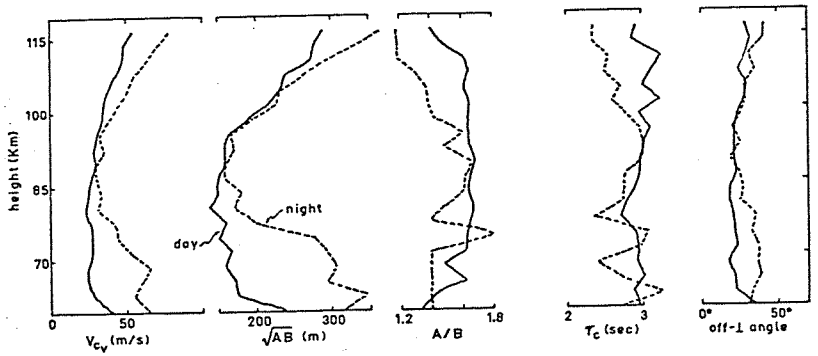

Figure 5.3 As in Figure 5.2, but for October 1976.

hourly value with the number of determinations in the hour, however this gave virtually the same results, and so is not shown. The values are plotted at the height corresponding to the centre of the scattering volume. It should be noted that there are problems with significant figures in the median ratio value- viz. it tends to be 'quantized'. This is strictly a computational effect, and also occurs to a lesser extent in the characteristic time.

The August recording period was plagued with thunderstorms, and although the analysis (Appendix C) does attempt to correct the correlations for noise, there may be some residual effects, especially at night. An examination of the day values shows that the paatern scale increases more or less smoothly with height above ~90 Km. This suggests that the echoes are actually coming from different (virtual) heights, which may mean that the local E region is rather 'patchy', since one one would expect total reflection at about 105 Km (~110 Km virtual height) for our frequency (2.22 MHz.) in the day. The day-night pattern parameters ($\sqrt{AB}$, A/B, τ_c) tend to agree better in the meteor region (~85-100 Km) which suggests that many of the fading patterns here may be related to meteor trails. The patterns are seen to be preferentially aligned perpendicular to the drift direction, especially in the day. The more random alignment at night may be due to poorer data, or could be due to preferential alignment along some constant direction. The data have not been examined for this possibility as yet.

Figure 5.3 shows October data analysed for the large triangle,

to compare with August data. There are major differences in the day-night changes. The similarities are the increase in pattern scale with height, the lack of change between day and night in the meteor trail region, and the low off-⊥ angles. The presence of data at lower heights is due to seasonal changes.

Figure 5.4 shows October data analysed for the small triangle. Compared with this are the C.R.C. data, and Adelaide data. The U of S data were analysed as in Appendix C (unweighted fit), the C.R.C. data with the weighted fit (section C.7), and the Adelaide data with their own analysis (A.H. Manson, private communication). The C.R.C. data (58-98Km) were combined to give six height ranges, and the Adelaide data (81-93Km) to give a single value. The Adelaide values for the plotted parameters were calculated directly from single medians for A (major axis), A/B, V_c, and off-⊥ angle, and dimensioned quantities were divided by 1.18 before plotting. Differences between weighted and unweighted fits have been discussed in Appendix B, viz. the weighted fit gives larger pattern scales (~10%) and larger axial ratios (~6%). These differences should be kept in mind when comparing U of S and C.R.C. values. There are also other biases apparently depending on lag step, etc. Thus the major difference, and probably the only significant one, is the greater U of S axial ratios above ~80 Km. So why is the fading rate at Ottawa lower, as mentioned in Chapter 2? It may depend on velocity values, which seems unlikely, or it could be that the shape of the auto correlation is different, since the fading rate was calculated from the value at 1 lag, assuming a Gaussian

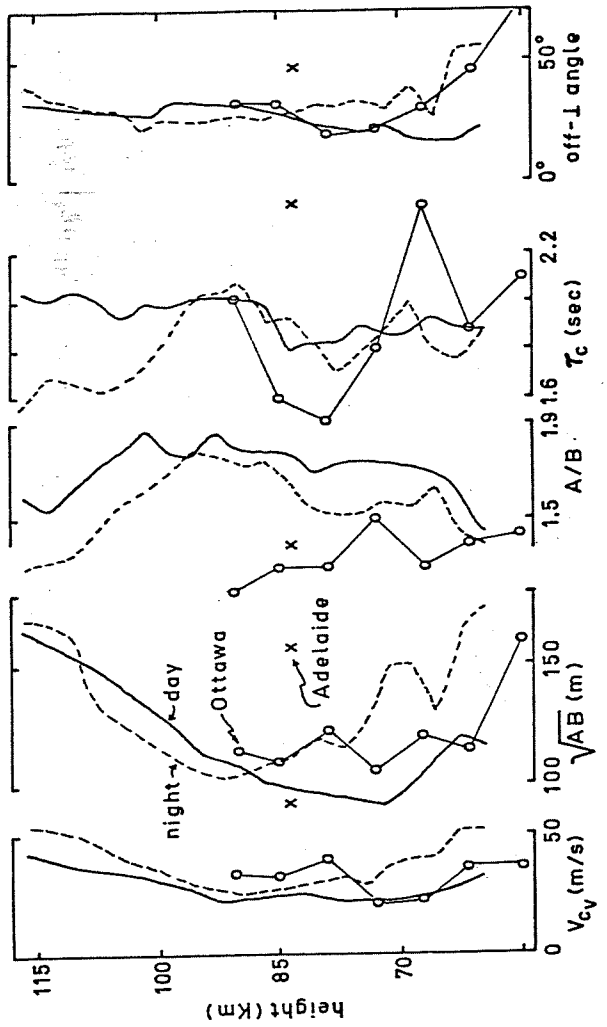

Figure 5.4 Median pattern parameters (ρ=0.61) for October 1976 (Saskatoon) using small triangle (156 m), day ——, night ----. Also data from Ottawa (winter, noon) —o—o— , and Adelaide (summer, day) X.

shape. It can also be seen that the patterns for U of S (day and night) and C.R.C. data are both preferentially aligned perpendicular to the drift direction.

The Adelaide data show much larger pattern scales and larger characteristic times. This could be due to seasonal differences (see Stubbs, 1977). Their off-⊥ angles are almost completely random (median=45°),which suggests some difficulty with the analysis method or program.

A final figure, 5.5, compares large and small triangle pattern parameters for October 1976. Ratios, large to small, are shown. A similar comparison had been shown in Figure 3.15 for a small amount of data, in which only those records which could be analysed for both the large and small triangles were used. The pattern scale and characteristic time differences are larger here, which probably means that, on the average, the use of small antenna spacing permits the analysis of data with smaller pattern scales and characteristic times than the large spacing.

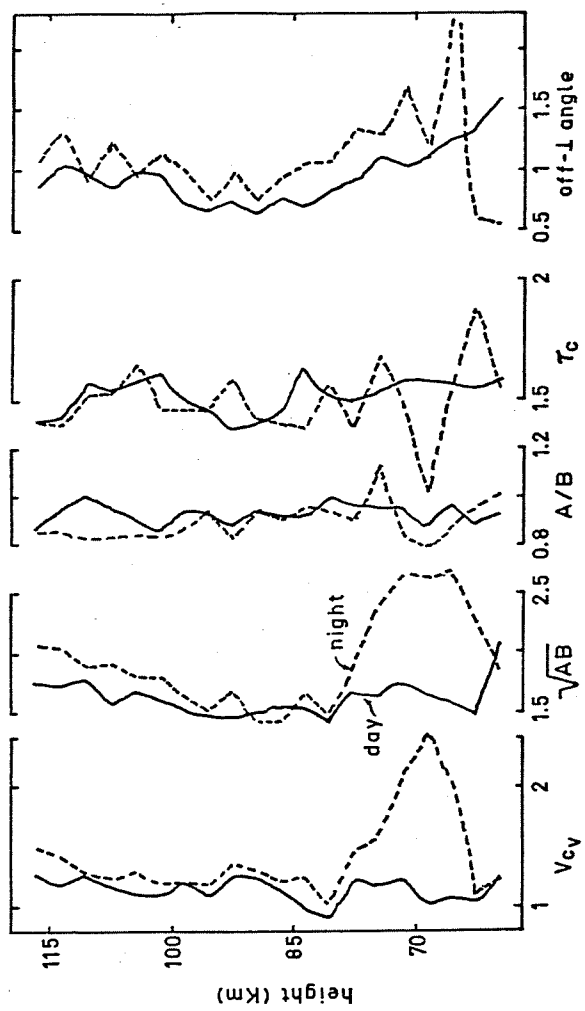

Figure 5.5 Ratios of median pattern parameters (large to small triangle values) for October 1976 (Saskatoon).

CHAPTER VI

EFFECT OF ANTENNA COUPLING ON DRIFT AND PATTERN PARAMETERS

6.1 Introduction

The reson for an investigation of the effect of coupling is that our location seems to require very close antenna spacing for reasonable results. Even with the simulated small triangle, the NTD distribution is worse than at Ottawa or Adelaide. This is at least partly due to the spurious peaks in the cross correlations, but could also be due to the existence of still smaller pattern scales than we can now measure, or alternatively to changes in statistics (e.g. drift velocity) over the area of our present antenna system. A single equilateral triangle with even smaller spacing ($\sim 1\lambda$, 135m) is now under construction. Although the coupling in the present system appears to be negligible, possibly due to the use of a pair of spaced dipoles for each receiving antenna, this might not be the case for the new system, in which single similarly aligned dipoles will be used.

Work has been done in the past by Fedor and Plywaski (1972) on the effect of coupling in a one dimensional situation. They have used complex correlations (phase included) between signals received at two antennas. This permits the use of an arbitrary phase in the coupling coefficient without the necessity of starting with model fading sequences; viz., the complex correlation can be modified directly according to the assumed phase

shift between antennas. The assumption of constant zero phase difference between signals must be used, which does not apply in practice, but is a reasonable first approximation. They have also assumed statistical differences between fading at different antennas, which is unrealistic on the average. The results are of limited value, since most workers correlate amplitudes, not complex signals. However, their values have been checked for the cases in which the phase of the coupling coefficient is suitable (0°, or 180°) for the application of amplitude correlation; i.e. a fraction of the amplitude at one antenna is added to, or subtracted from, that at another.

This chapter will discuss two dimensional effects.

6.2 Method of computation.

The method is to set up model correlations for a given set of pattern and drift parameters; work out the resulting correlations when coupling is included; and then use the 'Poor man's FCA' analysis (Appendix D) to deduce the modified FCA parameters. As stated previously, unless fading sequences are generated, 'coupled' with some arbitrary phase relation, and then correlated, we are restricted to 'in phase' or 'out of phase' coupling; since otherwise the problem becomes non-linear. This is not a serious drawback, since 0° or 180° phase shifts in the coupled signal are expected to have the greatest effect on the correlations, but creates a difficulty in simulating a given antenna system.

Calculations by Fedor and Plywaski (1972) indicated that

half wave dipoles suspended $\frac{1}{4}\lambda$ above the ground and spaced at 1λ have an isolation of ~20 dB (phase relations were not shown), and so this value will be used for the following work.

Since coupling is essentially instantaneous, the correlations will be modified around zero lag, and there may be a secondary peak here if the 'actual'peaks are at large lag (e.g. low drift speed), or even a primary peak if the coupling is very strong and the 'actual' peaks small.

A basic assumption made is that the fading at the three antenna positions (no coupling) is statistically equivalent (mean, s.d., auto correlation). Then if X(t), Y(t), and Z(t) are the 'actual' amplitudes at the ground; and A(t), B(t) and C(t) are the measured amplitudes (with coupling):

$$\left.\begin{aligned} A &= X + \Delta_1 Y + \Delta_2 Z \\ B &= Y + \Delta_1 X + \Delta_3 Z \\ C &= Z + \Delta_2 X + \Delta_3 Y \end{aligned}\right\} \qquad \ldots.(6.1)$$

where Δ_1, etc. are the coupling coefficients (+ve for in-phase).

Let $\mu_x = \mu_y = \mu_z = 0$, and $\sigma_x = \sigma_y = \sigma_z = 1$ (mean and s.d.). then $\mu_A = \mu_B = \mu_C = 0$, and

$$\sigma_A^2 = 1 + \Delta_1^2 + \Delta_2^2 + 2\Delta_1 \rho_{XY}(0) + 2\Delta_2 \rho_{XZ}(0) + 2\Delta_1\Delta_2 \rho_{YZ}(0) \qquad \ldots.(6.2)$$

etc., where $\rho_{XY}(0)$ is the 'actual' cross correlation between X(t) and Y(t) at zero lag; and

$$\rho_{AB}(\tau) = \left\{ \rho_{XY}(\tau) + (2\Delta_1 + \Delta_2\Delta_3)\rho_{XX}(\tau) + \Delta_3\rho_{ZX}(-\tau) + \Delta_1\Delta_2\rho_{ZX}(\tau) + \Delta_1\Delta_3\rho_{YZ}(\tau) + \Delta_2\rho_{YZ}(-\tau) + \Delta_1^2\rho_{XY}(-\tau) \right\} / (\sigma_A\sigma_B) \qquad \ldots.(6.3)$$

etc. are the cross correlations, where $\rho_{XX}(\tau)$ is the (common) auto correlation of the 'actual' fading.

The derivatives of the cross correlations can be found by differentiating equations 6.3, and a zero search is done to find the lag for maximum. Since all 'measured' correlation functions are given directly by formulas, the required parameters for PMFCA are easily found. Note that the peaks do not now satisfy NTD=0 (neither are the correlations strictly Gaussian), so that the full PMFCA solution (including rejection for NTD>0.3, and the weighted least squares fit) must be used.

The original ('actual') correlations, $\rho_{XY}(\tau)$, $\rho_{XX}(\tau)$, etc., are, of course, defined by the initially chosen FCA parameters V, ϕ, A, B, θ, and C. In order to obtain representative FCA parameters, random distributions roughly based on previous experimental results (except for tilt angle) were used to generate sets of parameters as follows:

$$\left.\begin{aligned} V &= 150r^3 + 20 && \text{true } \underline{\text{pattern}} \text{ velocity} \\ A &= 80 + 220r^2 && \text{major axis} \\ B &= A/(1+3r^2) && \text{minor axis} \\ C &= 3r^{1.5} + 1 && \text{char. time} \\ \theta &= \pi r && \text{tilt angle(of A)} \\ \phi &= 2\pi r && \text{drift direction} \end{aligned}\right\} \qquad \ldots.(6.4)$$

where the r's are independent, uniformly distributed, random numbers between 0 and 1.

6.3 Results.

Figure 6.1 shows the antenna system used (equivalent to the simulated small triangle, spacing 1.15λ). Figure 6.2 shows some results for $\Delta_1=\Delta_2=\Delta_3=$ 0.1 (20 dB isolation; in-phase coupling between pairs of antennas). The results show that the pattern scale is increased, as might be expected, because the fading looks more similar at all antennas with coupling. The true speed is increased by a factor of~1.2 on the average. The axial ratio shows only a minor increase. The characteristic time is decreased, which means that coupling 'creates' greater internal time change in the pattern. The latter is rather hard to explain physically. The interesting result is that, for small axial ratios (near isometric patterns), the direction of elongation becomes more nearly perpendicular to the drift direction.

A second calculation used the coupling coefficients $\Delta_1=$ 0.1, $\Delta_2=\Delta_3=0$. That is, the antenna pair oriented in the direction 30° E of N is strongly coupled, but the other pairs are not. It is difficult to say at present whether this is reasonable in practice, however it is probable that there will be some differences in coupling depending on the dipole orientation with respect to the direction of the antenna pair. Different sets of FCA parameters have been used (a smaller number, but with the same distributions).

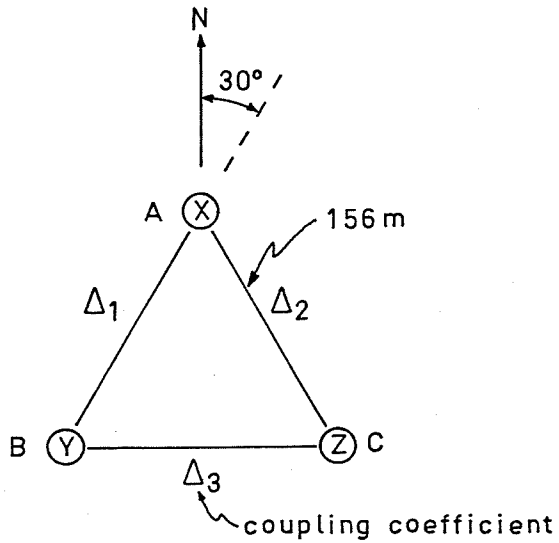

Figure 6.1 Antenna system used in coupling calculations.

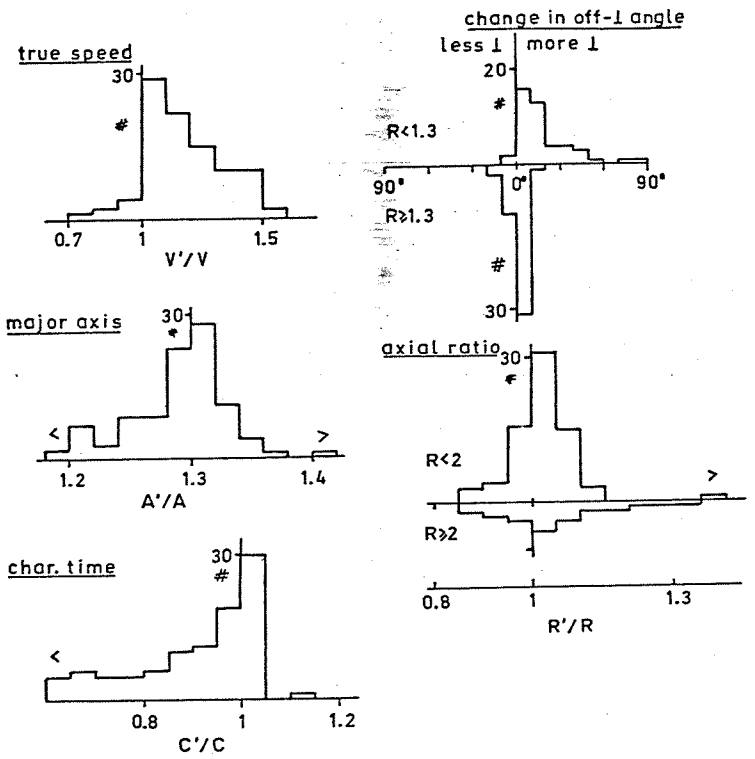

Figure 6.2 Effect of equal, in phase, coupling between all antennas (20 dB isolation). Histograms of ratios of coupled (primed) to uncoupled values given (except for off-⊥ angle).

Figure 6.3 compares 'actual' and 'measured' parameters. It can be seen that the pattern scale and true speed are increased by a small amount on the average, the axial ratio is increased by a factor of about 1.2, the characteristic time is decreased, as before, but by a smaller amount, and the off-⊥ angle is modified more or less randomly (greater changes for smaller axial ratios). However, the tilt angle for small axial ratios is very preferentially aligned along the direction of the coupled antenna pair. This might have been expected for in-phase coupling (and maybe the opposite for out of phase coupling) because the pattern will look more similar in these two antennas, which would be interpreted as elongation in this direction. This latter result, when compared with the data of Keneshea et al. (1965), in which a preferred alignment along the direction of one antenna pair was found, suggests that there may have been strong coupling present; although no obvious reason for preferential coupling is evident from their description of the antenna system.

The drift directions have not been compared in either calculation because these were found to be virtually unaffected ($<10^{\circ}$) by coupling, although agreement is a little better with equal coupling.

6.4 Conclusions.

Although changes in parameters have, for the most part, been shown as single histograms, it is fairly clear that the magnitudes of the modifications to parameters depend rather

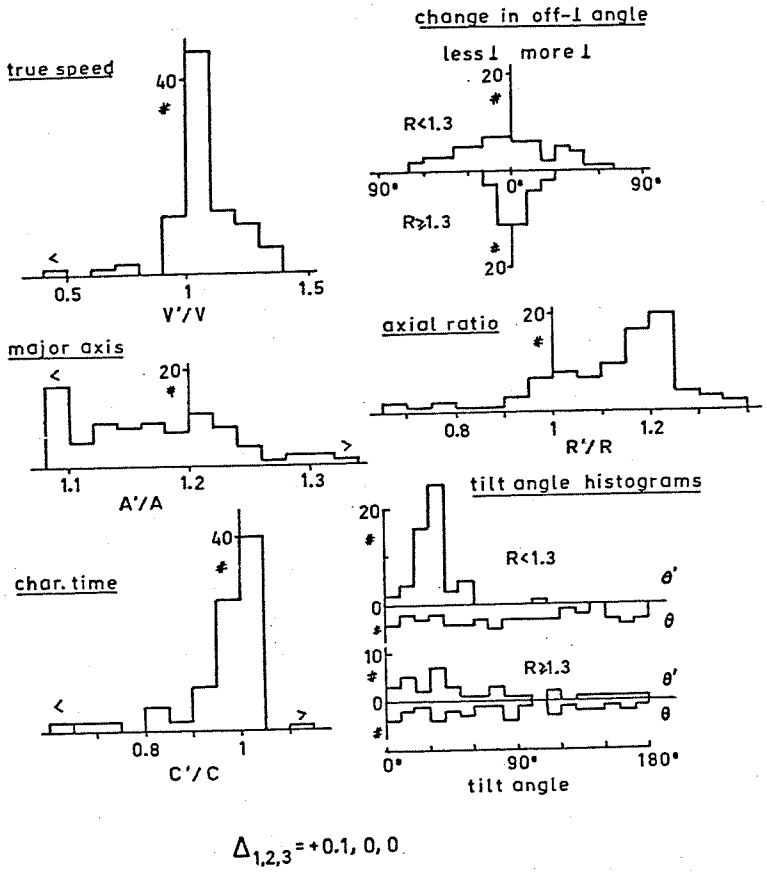

Figure 6.3 Effect of unequal coupling. Only one pair of antennas is coupled (20 dB isolation). Values with coupling are primed.

strongly on the actual parameters, especially when the coupling is unequal. For example, if the actual pattern is elongated along a pair of antennas which are strongly coupled, the axial ratio may increase, whereas if the alignment is perpendicular it may decrease, and so on. Also, if there is equal coupling (in phase) between antennas, and the actual pattern has no preferred direction of elongation, a statistical analysis of tilt angles might indicate three preferred directions (along each antenna pair); or if one pair is coupled more strongly than the others, then one preferred direction. Since this has not been seen in Chapter 5, where elongation was found to depend on drift direction (for both large and small spacing), there is additional indication that coupling is not important with the present antenna system.

REFERENCES

Briggs,B.H.	1967	Instruction Manual for Drifts ADP42, Dept. of Physics, Univ. of Adelaide.
Briggs,B.H., G.J. Phillips and D.H. Shinn	1950	Proc. Phys. Soc. B63, 106
Briggs,B.H., and M. Spencer	1955	'The Physics of the Ionosphere', pg. 123, Phys. Soc. (London)
Chandra,H., and B.H. Briggs	1976	'The Effect of Filtering on Ionospheric Drift Parameters Determined by Full Correlation Analysis', paper presented at conference, Townsville, Australia.
Fedor,L.S.	1967	J.G.R. 72, 5401
Fedor,L.S., and W. Plywaski	1972	J.A.T.P. 34, 1285
Felgate,D.G., and M.G. Golley	1971	J.A.T.P. 33, 1353
Golley,M.G., and D.E. Rossiter	1970	J.A.T.P. 32, 1215
Gregory,J.B., and A.H. Manson	1975	J. Atmos. Sci. 32, 1667
Gregory,J.B., and C.E. Meek	1976	'Determination of Winds in the Lower Ionosphere', Final report on D.S.S. contract 01SU.36100-5-0297 , Institute of Space and Atmospheric Studies, University of Saskatchewan.
Hoel,P.G., S.C. Port, and C.J. Stone	1971	'Introduction to Statistical Theory', Houghton Mifflin Co. (Boston).
Keneshea,T.J., M.E. Gardner, and W. Pfister	1965	J.A.T.P. 27, 7
MacDougall,J.W.	1966	J.A.T.P. 28, 1093
Manson,A.H., J.B. Gregory, and D.G. Stephenson	1974	J. Atmos. Sci. 31, 2207

REFERENCES- cont'd

Meek,C.E.	1977	'Comparison of Wind and Electron Density Variations in the Mesosphere', Ph.D. thesis, University of Saskatchewan
Mitra,S.N	1949	Proc. Inst. Elect. Engrs., Pt.III, 96, 441
Pfister,W.	1971	J.A.T.P. 33, 999
Phillips,G.J., and M. Spencer	1955	Proc. Phys. Soc. B68, 481
Pütter, Von P. St.	1954	Proc. Camb. Conf. Phys. Ionos. pg. , Phys. Soc. (London)
Sprenger,K. and R. Schminder	1969	J.A.T.P. 31, 1085
Stubbs,T.J.	1977	J.A.T.P. 39, 589
Wright,J.W.	1974	J.A.T.P. 36, 721

APPENDIX A

FOOTNOTES

A.1 Weighted least squares fit to times.

If the antenna pairs are defined by (d_i, ψ_i), where the time delay t_i (given by the position of the maximum in the cross correlation) is taken to be positive if it indicates pattern motion in the direction ψ_i; then the delays for a particular apparent velocity (V_a, ϕ_a) are given by:

$$t_i = \frac{d_i}{V_a} \cos(\psi_i - \phi_a)$$

$$= \frac{\cos\phi_a}{V_a} (d_i \cos\psi_i) + \frac{\sin\phi_a}{V_a} (d_i \sin\psi_i) \quad .$$

Let

$$\beta = \begin{bmatrix} \frac{\cos\phi_a}{V_a} \\ \\ \frac{\sin\phi_a}{V_a} \end{bmatrix}, \quad Y = \begin{bmatrix} t_1 \\ \cdot \\ \cdot \\ \cdot \\ t_n \end{bmatrix}, \quad X = \begin{bmatrix} d_1\cos\psi_1 & d_1\sin\psi_1 \\ \cdot & \cdot \\ \cdot & \cdot \\ \cdot & \cdot \\ d_n\cos\psi_n & d_n\sin\psi_n \end{bmatrix} .$$

Let ρ_i be the peak values of cross correlation (at delay t_i). Usually there will be only n=3 pairs of antennas involved. Then the solution for a least squares fit of apparent velocity to the time delays is (e.g. Hoel et al.,1971, Ch.4):

$$\beta = (X^T X)^{-1} X^T Y$$

This solution minimizes the squared error in the time delays, which is:

$$\Sigma e^2 = (X\beta - Y)^T (X\beta - Y).$$

If X and Y are modified according to:

$$x_{ij} = x_{ij} \rho_i$$

$$y_i = y_i \rho_i$$

before solving for β, the squared error in time delays is effectively weighted by ρ_i^2. A similar procedure applies to weighting of the FCA fit mentioned in section C.7, except that x_{ij} and y_i are multiplied by ρ_i^2.

A.2 Cross spectral analysis of fading records.

Figure A.1 shows spectra of fading sequences, and coherence and phase between spectra. A five point block filter has been used on both power and cross spectra. Enhanced energy occurs in all antennas near 0.2 Hz, indicating a weak wave-like pattern embedded in the normal 'random' fading. The initial reason for this type of analysis was to try to obtain delay times from the phase relationships between fading sequences. The plot shows the phase difference versus frequency for the smoothed cross spectra, and the expected variation (straight lines) determined by the delays measured from the peaks of the cross correlations. A fair amount of imagination is needed to see that the straight lines fit the plotted phase difference points, and especially to see where 'wrap-around' occurs. On the basis of this record, the use of cross spectral analysis in determining delays does not seem feasible. Similarly poor results were obtained on the same record for greater smoothing of the cross spectra.

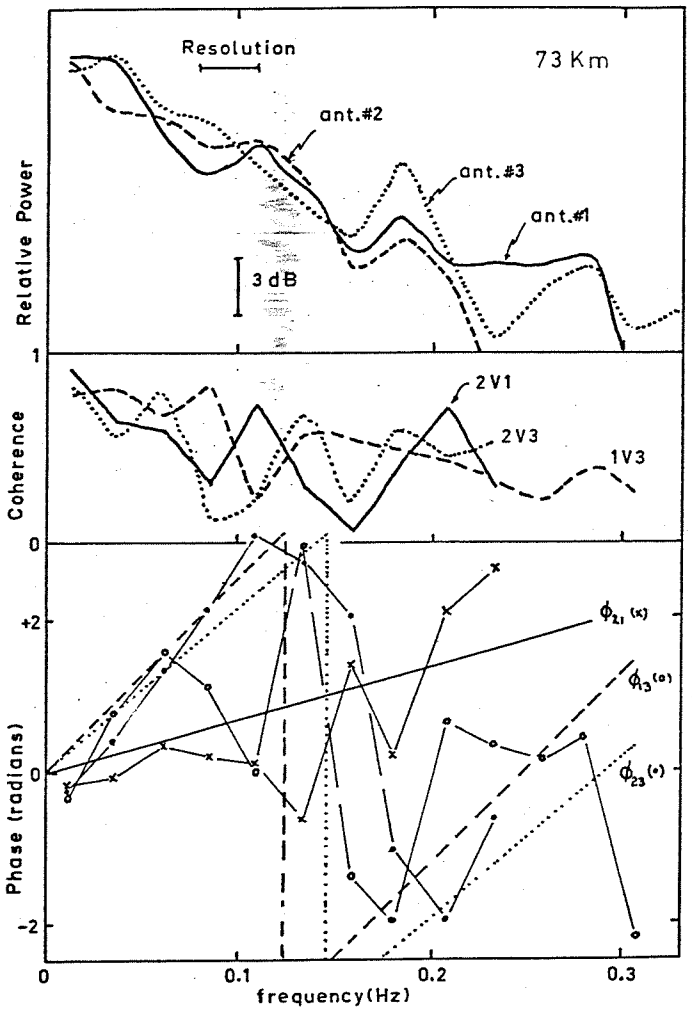

Figure A.1 Illustration of results of cross spectral analysis of fading records (large triangle). Bottom panel compares phase vs. frequency variation predicted from delays of peaks in cross correlations (straight lines ——, -----, ...) and that calculated directly by spectral analysis (joined points).

A.3 FCA results in the meteor trail region.

Figure A.2 shows hourly mean winds from the October 1976 ten day run. The semi-diurnal tide is clearly evident, which suggests that, although meteor trails have been found to perturb the apparent velocity, the true velocity does not suffer any serious modification.

A.4 Example of the method of zero NTD.

An example of a contour plot of the average cross correlation for NTD=0 is shown in Figure A.3 (a negative value is represented by '-', 0.1 by '1' etc.). The peak, which presumably indicates a pattern motion, is circled. Since $t_{12}+t_{23}+t_{31}=0$, the t_{31} axis (not shown) is diagonal, down to the right. This type of plot is only available, without interpolation of the cross correlation sequences, if the cycling is such (e.g. 3 antennas) that the corrections to the lags for cycling time also add up to zero. In practice, a plot was usually not generated, and correction for cycling time was made after the exact times for the peak, by paraboloid fit, had been found. The apparent velocity was then calculated.

The plot is still of interest, however, since each pattern motion (if more than one) is represented as a separate peak. Note that each 'ridge' (horizontal, vertical, diagonal) stands for a peak in a single cross correlation. The method is not foolproof in that a particularly large peak in one cross correlation will create many separate peaks along the 'ridge'. If all the fading is assumed to be due to pattern motions, then

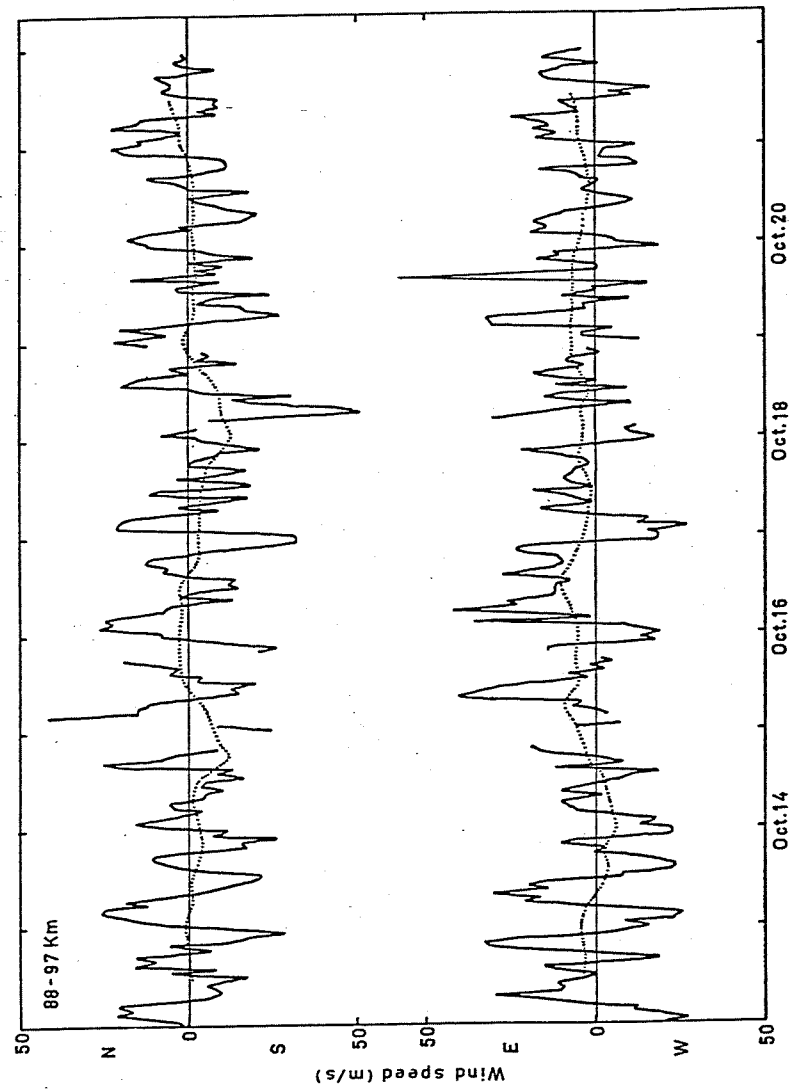

Figure A.2 Raw hourly mean winds from Oct '76 ten day run (solid line) and mean wind after removing tidal components (dotted line).

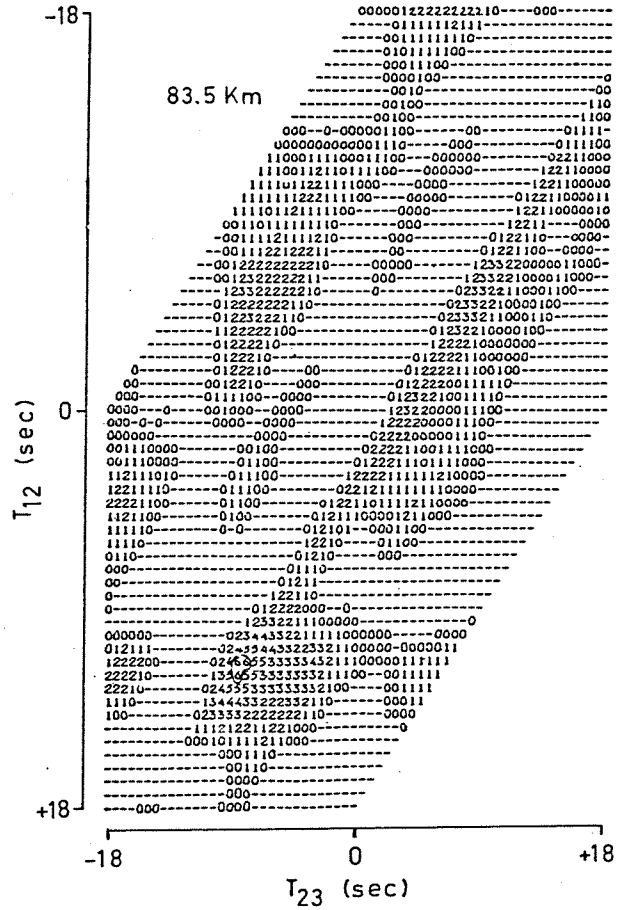

Figure A.3 Illustration of method of zero NTD. Each point represents the average correlation (0.2 = '2', negative value = '-', etc.) for a set of lags for which NTD is zero. The lags for the maximum value (circled) are used to calculate (apparent) drift velocity.

this may not be an unrealistic picture.

APPENDIX B

EFFECTS OF MINOR CHANGES IN ANALYSIS ON FCA PARAMETERS

B.1 Introduction

The following data came from the four antenna system (Figure 1.1). 760 amplitudes are measured at each antenna for a given height. The spacing is 4/15 sec. These are generally averaged to reduce computation time. The data are grouped according to data set analysed, and different groups should not be compared.

Comparisons are made between large and small antenna spacing, recording rate, amount of raw data averaging, and weighted vs. unweighted least squares fits in the FCA method (Appendix C).

B.2 Large and small antenna spacing and sample rate.

Table B.1(a) compares the large and small triangle output. Both used data averaging in 2's (resulting in a lag step of 8/15 = 0.533 sec) and the unweighted fit to the correlations. Also shown are values for ½PRF on the small triangle, i.e. every second amplitude is discarded and there is no averaging of data; the lag step is still 0.533 sec. The ½PRF values use the weighted fit, however. Instead of plotting the full $\Delta\phi$, and $\Delta V/V$ distributions, as was done in Chapter 3, a single point from these is used for comparison. It can be seen that the quality and quantity of output from the large triangle are much lower than that from the small. The reason for the degradation in quality is not known. The ½PRF data shows a small

loss in quantity, and maybe a very minor loss in quality. The improvement in the $\Delta V/V$ distribution and the changes in FCA parameters can be attributed to the weighting (see section B.5). Thus this lower recording rate is quite feasible; the saving would be in data storage, not analysis, since the cross correlations must still be calculated to the same maximum lag.

B.3 Amount of averaging, small triangle.

Table B.1(b) shows the results of different amounts of averaging (which also change the lag step). There are only minor changes in pattern parameters, but the quality is seen to be much worse with increased averaging. It was also mentioned in Chapter 2 that the quality of smoothed data was lower.

B.4 Amount of averaging, large triangle.

More averaging also degrades the quality here (Table B.1(c)), although not by much, but gives a little more output data. The pattern scale increases by ~10% as does the characteristic time, but the axial ratio decreases. Similar, but smaller changes were also seen in (b), which suggests that these are real effects, not just statistical variations. The sense of the changes in parameters is the same as that predicted for increased low pass filtering in Appendix E (Figure E.3), but the actual changes shown here are much greater. This might be due to the difference in lag step in conjunction with the type of analysis, but the difference in the low pass filter (i.e. Gaussian weights vs. block average) may also play a part.

B.5 Weighted vs. unweighted fit.

Comparison between the unweightd fit, which has been used in Chapter 3, and the intuitively better weighted fit (see section C.6) on small triangle data (Table B.1(d)) shows that the quality, as given by the $\Delta V/V$ distribution, is increased by weighting. This is presumably due to better determination of V, since the $\Delta\phi$ distributions are approximately the same. The pattern becomes more elongated, but the characteristic time is unchanged by weighting. An additional parameter, the median drift speed (over all heights) is also listed, since it is representative of the change occurring at each height. Thus, weighting seems to increase the calculated speed by ~20%. Further discussion on this point is contained in Appendix D (section D.4). Quantities of output are not shown because they are virtually the same. The only possible rejection difference depends on whether the fitted ellipsoid is real (i.e. a,b,c real) or not.

Table B.1 Comparison of FCA output for minor changes in analysis.

Group	Ant.	Anal.	Avg.	Adj. hts. % occurrence		Adj. times % occurrence		median pattern param.				%FCA
				$\Delta\phi<30°$	$\Delta V/V<30\%$	$\Delta\phi<30°$	$\Delta V/V<30\%$	A	B	τ_c	A/B	
(a)	L	unwt'd	2	44	35	46	44	195	117	2.84	1.8	33
	S	unwt'd	2	69	61	76	68	132	73	2.15	1.8	51
	S	$\frac{1}{2}$PRP wt'd	1	63	60	73	72	147	67	2.14	2.2	48
(b)	S	unwt'd	2	66	54	70	63	155	103	2.2	1.5	72
	S	unwt'd	3	56	40	64	41	160	108	2.45	1.4	65
(c)	L	unwt'd	2	51	41	44	37	210	123	2.7	1.8	37
	L	unwt'd	3	56	36	40	34	218	132	3.05	1.6	41
(d)	S	unwt'd	2	71	70	86	83	116	63	2.14	1.9	25
	S	wt'd	2	72	76	89	88	127	56	2.18	2.2	33

V(med.)

APPENDIX C

WIND ANALYSIS METHOD

C.1 Introduction

This appendix describes the present full correlation analysis method based on the discussion in Chapter 3. The numerical criteria quoted are probably close to optimum for our ionospheric conditions, since they have been based on extensive examination of data. The basic ideas behind each criterion apply to any such measurement. However, such a careful treatment may not be required at other locations.

C.2 Preliminary rejection criteria

Preliminary rejection criteria on the raw fading sequences are that the standard deviation should be of reasonable size, and if it is suitable, then the fading rate, determined from the width of the auto correlation, should be relatively low. Generally, the latter criterion is that the auto correlation should not fall below 0.6 by a lag of 0.6 sec, although this limit has been changed in some cases.

The above criteria are intended to exclude very noisy data, cases of no signal, or cases of fast interference fading between several strong echoes. Initial rejection of these data is important because the calculation of cross correlations which follows is the most expensive part of the analysis. Signals have not been specifically rejected for overloading, although this is available on the output cards, since some

evidence has been seen which indicates that the velocity values are not affected (although pattern parameters are) in the present analysis.

C.3 Reduced maximum lag

The cross correlation sequences are then calculated to a maximum lag determined by the season (see section 3.3.5). At this point, enough information is available for the choice of a more reduced maximum lag, beyond which no peaks are expected (see section 3.4.7). A more economical method would have found the limited lag first, from the cross correlations at zero lag, and then calculated the correlations within this limit; but the saving in terms of the whole analysis might only be of the order of 10%, especially since often, choice of a more limited lag is not possible in our data.

C.4 Choice of cross correlation peaks.

At this point there are three cross correlation sequences (for either of the two antenna systems employed) corresponding to three pairs of antennas aligned along different directions. A significant peak in a cross correlation sequence will be defined to be a local peak which has a value greater than 0.1. Accurate locations (in lag) and magnitudes of these are determined for all three sequences by a parabolic fit around the peak value. The greatest peak in each sequence is called the primary peak, and the others, secondary peaks. If there is no

significant peak in at least one sequence, the analysis is terminated.

The numbers of peaks are reduced by combining those which differ in lag by less than 20% (the maximum of the two is retained), and by rejecting any secondary peaks which are less than the primary peak in the sequence by a factor of 1.8. Then a search, based on the N.T.D., is done to see whether any combination of peaks, one in each sequence, could refer to a pattern motion. Generally, the more doubtful the data (i.e. the more secondary peaks), the more stringent is the N.T.D. limit. The possibilities have been divided into four classes, and each is dealt with differently. These are now defined. It is useful to refer to Figure 3.9, where some of these types were illustrated.

a) One significant peak in each sequence

The N.T.D. is calculated from the accurate peak locations (time lags) found above, and the analysis is terminated if this is greater than 0.3. Otherwise, FCA is attempted (see section C.5).

b) One peak in each of two sequences and two peaks in the other.

The N.T.D. is calculated for each of the two combinations and if a value less than 0.2 is found, then this set of peaks is used in section C.5. Otherwise the analysis is terminated.

c) One peak in each of two sequences and three or more peaks in the other.

In this case, the position at which the peak should occur in the doubtful sequence is calculated from the peaks in the good sequences by N.T.D.=0. The calculated position must be within maximum lag and the correlation value at this position must be greater than 0.1. If these conditions are met, FCA is attempted, since it is likely that the chosen position is near a peak. The least squares fit uses several points on either side of the specified location, and so the 'correct' peak will probably be included in the analysis.

d) More than one peak in two or more sequences

These are very doubtful data since there may be many combinations of peaks with a low N.T.D. However, if the N.T.D. of the primary peaks is less than 0.1, FCA is attempted.

C.5 Selection of points for the least squares fit and correction for noise.

The exact positions (by parabolic fit) of the peaks, calculated before, are not used here; rather the index positions for local maxima in the cross correlation sequences are employed. These index positions, corresponding to the final chosen peaks, have been saved in the previous selection.

The present criteria used for selection of correlation 'observations' follows. A maximum of four points are taken from the mean auto correlation (up to the lag where it falls below 0.2) and a maximum of seven points from each cross correlation, centred on the peak position. All cross correlation values are required to be greater than 0.1, and greater than

one third of the corresponding peak value. There must be at least two suitable points from each cross correlation. If these conditions are not met, the analysis is terminated.

Here, the data are checked for noise. A least squares fit of a Gaussian to the mean auto correlation, leaving out zero lag, is made. If the extrapolated value at zero lag is much less than 1, then random noise is present in the data. A rough correction for this involves multiplication of all correlation values by a factor which makes the extrapolated value equal to 1.

C.6 Least squares fit.

This is most easily done by converting the function to be fitted to the data into linear form. Then standard matrix techniques are used to find the coefficients for a best fit. The correlation function (equation 3.10) is:

$$\rho(r,s,t) = \exp\left(-\tfrac{1}{2}\left[\frac{(r\cos\theta + s\sin\theta - V\cos\phi' t)^2}{a^2} + \frac{(-r\sin\theta + s\cos\theta - V\sin\phi' t)^2}{b^2} + \frac{t^2}{c^2}\right]\right) \qquad \ldots(C.1)$$

This is expanded into the linear form:

$$-2\ln\rho = \beta_1 r^2 + \beta_2 s^2 + \beta_3 rs + \beta_4 rt + \beta_5 st + \beta_6 t^2 \qquad \ldots(C.2)$$

where $\beta_1 = \frac{\cos^2\theta}{a^2} + \frac{\sin^2\theta}{b^2}$, $\beta_2 = \frac{\sin^2\theta}{a^2} + \frac{\cos^2\theta}{b^2}$

$\beta_3 = \frac{\sin 2\theta}{a^2} - \frac{\sin 2\theta}{b^2}$, $\beta_4 = 2V\left(-\frac{\cos\phi'\cos\theta}{a^2} + \frac{\sin\phi'\sin\theta}{b^2}\right.$

$$\beta_5 = 2V\left(-\frac{\cos\phi'\sin\theta}{a^2} - \frac{\sin\phi'\cos\theta}{b^2}\right) ,$$

and $$\beta_6 = V^2\left(\frac{\cos^2\phi'}{a^2} + \frac{\sin^2\phi'}{b^2}\right) + \frac{1}{c^2} , \qquad ...(C.3)$$

and the parameters r,s, and t are chosen for each observation of correlation. A choice of the coefficients β_i, i=1,2,...,6 is required which will minimize the squared error:

$$\sum e^2 = \sum_1 \left[2\ln\rho_i + \beta_1 r_i^2 + \beta_2 s_i^2 + \beta_3 r_i s_i + \beta_4 r_i t_i + \beta_5 s_i t_i + \beta_6 t_i^2\right]^2 \qquad ...(C.4)$$

The solution is most easily represented in matrix notation as follows (e.g. Hoel et al., 1971, pg.122).

Let

$$\boldsymbol{\beta} = \begin{bmatrix} \beta_1 \\ \vdots \\ \beta_6 \end{bmatrix} , \quad X = \begin{bmatrix} r_1^2 & s_1^2 & r_1 s_1 & r_1 t_1 & s_1 t_1 & t_1^2 \\ \vdots & & & & & \\ r_i^2 & \cdots & \cdots & \cdots & \cdots & t_i^2 \\ \vdots & & & & & \\ r_m^2 & s_m^2 & \cdots & \cdots & \cdots & t_m^2 \end{bmatrix} , \quad Y = \begin{bmatrix} -2\ln\rho_1 \\ \vdots \\ -2\ln\rho_i \\ \vdots \\ -2\ln\rho_m \end{bmatrix} \qquad ...(C.5)$$

where $\boldsymbol{\beta}$, X, and Y are the solution, parameter, and observation matrices, respectively. Then,for minimum squared error:

$$\boldsymbol{\beta} = (X^T X)^{-1} X^T Y \qquad ...(C.6)$$

The drift and pattern parameters are found from the elements of $\boldsymbol{\beta}$ according to the following equations.

$$\tan 2\theta = \frac{\beta_3}{\beta_1 - \beta_2} , \quad a = \sqrt{\frac{2}{\beta_1 + \beta_2 + \frac{(\beta_1 - \beta_2)}{\cos 2\theta}}}$$

$$b = \sqrt{\frac{2}{\beta_1 + \beta_2 - \frac{(\beta_1 - \beta_2)}{\cos 2\theta}}} ; \quad \tan\phi' = \frac{b^2(\beta_5\cos\theta - \beta_4\sin\theta)}{a^2(\beta_5\sin\theta + \beta_4\cos\theta)}$$

$$V = \frac{-\beta_5}{2\left(\frac{\cos\phi'\sin\theta}{a^2} + \frac{\sin\phi'\cos\theta}{b^2}\right)} , \quad \phi = \phi' + \theta$$

$$c = \sqrt{\frac{1}{\beta_6 - V^2\left(\frac{\cos^2\phi'}{a^2} + \frac{\sin^2\phi'}{b^2}\right)}} \qquad ...(C.7)$$

Note that the values of a,b, and c must be real, If they are not, the computed velocity is discarded. This is the same as the 'negative V_c^2' condition of Briggs et al.(1950).

C.7 Further comments

The least squares fit described in the previous section has minimized the squared error in $\ln\rho$. This weights the fit towards smaller values of ρ_i, which are likely to be less accurate. Therefore, a modification[1] of the analysis has been implemented which weights the squared error (equation C.4) by ρ_i^4. This corrects the above deficiency and gives additional weight to high values of ρ_i. Also, the auto correlations have been separately employed in the fit, which gives them relatively more numerical weight. The results of this improvement were that the consistency of the wind given by angle difference distributions did not change significantly, the vector difference distribution became better, and the final drift speed was greater by ~20% on the average. The reason for the latter

1. see Appendix A, section A.1

is not known.

C.8 Conclusions

The quantities of data passing and rejected by the various criteria are illustrated in Figure C.1. The data set consisted of 11 noon hours (October 1976 ten day run) recorded on the small triangle array. The amount of data recorded is not shown because the preliminary rejection by standard deviation and fading rate limits usually indicates lack of echoes, not poor quality data. The numbers of values are shown before and after each criterion applied. Rejected data is indicated by an arrow to the side.

There are not enough data output from the C.4(b), (c), and (d) 'channels' to see whether the quality (consistency of adjacent wind values) is as good as that from C.4(a), which is expected to give the least number of spurious values. However, this would be a very interesting comparison, and will be made in the future.

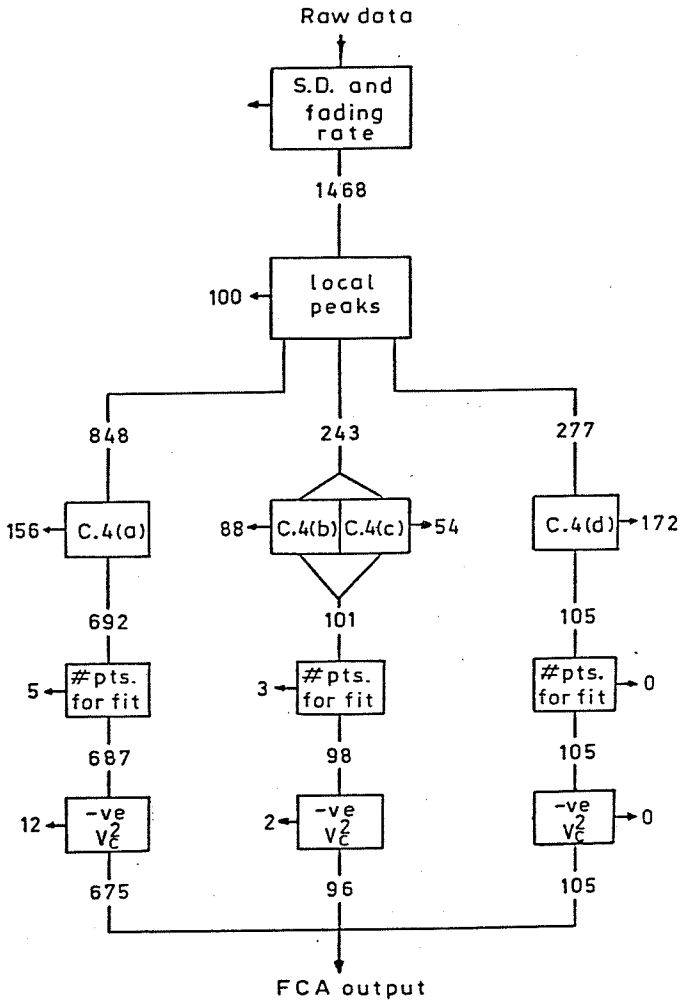

Figure C.1 Data rejection statistics for FCA analysis (Oct '76 ten day run, noon data, small triangle).

C.9 Quality and quantity statistics for day and night.

Table C. shows average statistics from the October 1976 ten day run for day (12-23Z) and night (0-11Z) using the previously described analysis (unweighted) on small triangle data.

Table C. Comparison of wind quality and quantity, day and night.

	%FCA	Quality				
		adj. hts. % occurrence		adj. times % occurrence		average
		$\Delta\phi<30^\circ$	$\Delta V/V<30\%$	$\Delta\phi<30^\circ$	$\Delta V/V<30\%$	# cards/hr
day	50	67	58	76	69	122
night	33	52	42	63	54	137

The # cards/hr refers to those data which passed the s.d. and fading rate criteria. The %FCA is the amount of FCA output with respect to this number. The amounts of data produced day and night are about equal, but the %FCA is much less at night and the quality is also lower. This is probably because many of the signals at night are due to interference from other radio sources, some of which must pass all the rejection criteria and produce spurious values of wind. Extensive examination of individual night records has not been done as yet, so various types of interference have not been categorized. Possibly a different set of rejection criteria would be useful here.

APPENDIX D

POOR MAN'S FCA

D.1 Introduction

This appendix derives a set of equations for determining FCA parameters from just the positions, t_{max_i}, and the values of the maxima, ρ_{max_i}, in the three cross correlations, and one point, (t_a, ρ_a), from the mean auto correlation. The assumptions are that the correlation function is Gaussian, and the N.T.D. is zero. Practical application will be discussed in section D.3.

D.2 Derivation of FCA solution

Figure D.1 describes the general antenna arrangement. The direction given to each pair defines the sign of t_{max_i}; i.e. a pattern moving in the direction of the arrow gives a positive delay.

The auto correlation is given by:

$$\rho(0,0,t) = \exp\left(-\tfrac{1}{2}\left[v^2\left(\frac{\cos^2(\phi-\theta)}{a^2} + \frac{\sin^2(\phi-\theta)}{b^2}\right) + \frac{1}{c^2}\right]t^2\right) \qquad \ldots(D.1)$$

Let
$$Q = v^2\left(\frac{\cos^2(\phi-\theta)}{a^2} + \frac{\sin^2(\phi-\theta)}{b^2}\right) + \frac{1}{c^2} \qquad \ldots(D.2)$$

Then
$$\rho(0,0,t) = \exp(-\tfrac{1}{2}Qt^2)\ , \qquad \ldots(D.3)$$

and Q can be found from one point on the auto correlation

$$Q = \frac{-2\ln\rho_a}{t_a^2} \qquad \ldots(D.4)$$

Table D.1 Numerical example of the Poor man's FCA

antenna parameters: d_i=156m, i=1,2,3; ψ_1=210°, ψ_2=90°, ψ_3=330°

input data	Solution
t_a=1.066sec	Q = 0.53
ρ_a=0.74	a = 97.4m
t_{max_1}=-2.05s, 2.84s, -.79s	b = 56.0m
ρ_{max_1}=0.17, 0.25, 0.31	θ = 158°
	V =16.6m/s (drift)
	ϕ = 90°
	c = 2.2s

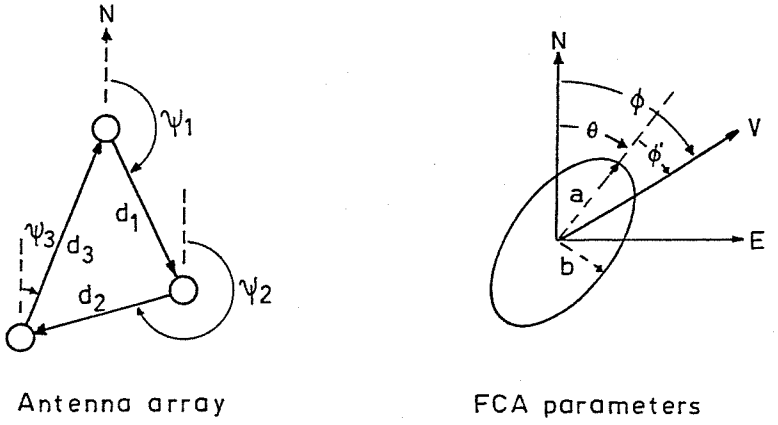

Figure D.1 Illustration of symbols used in derivation of the Poor man's FCA.

The cross correlations are given by:

$$\rho(d_i, \psi_i, t) = \exp\left[-\tfrac{1}{2}\left(\frac{(d_i\cos(\psi_i-\theta)-V\cos(\phi-\theta)t)^2}{a^2} + \frac{(d_i\sin(\psi_i-\theta)-V\sin(\phi-\theta)t)^2}{b^2} + \frac{t^2}{c^2}\right)\right] \quad \ldots(D.5)$$

where the antenna pair and direction are defined by d_i and ψ_i as shown in Figure D.1.

Then for the i^{th} antenna pair, t_{max_i} is found by setting the derivative of D.5 equal to zero.

$$t_{max_i} = \frac{Vd_i}{Q}\left(\frac{\cos(\phi-\theta)\cos(\psi_i-\theta)}{a^2} + \frac{\sin(\phi-\theta)\sin(\psi_i-\theta)}{b^2}\right) \quad \ldots(D.6)$$

This is substituted into D.4 to get ρ_{max_i}:

$$-2\ln\rho_{max_i} = d_i^2\left(\frac{\cos^2(\psi_i-\theta)}{a^2} + \frac{\sin^2(\psi_i-\theta)}{b^2}\right) - Qt_{max_i}^2 \quad \ldots(D.7)$$

Now define

$$m_i = \frac{-2\ln\rho_{max_i} + Qt_{max_i}^2}{d_i^2}$$

$$= \frac{1}{r^2b^2}\left(\cos^2(\psi_i-\theta) + \sin^2(\psi_i-\theta)r^2\right) \quad \ldots(D.8)$$

where r = a/b, and let $m_{ij}=m_i-m_j$.

Then the solution for the pattern parameters is:

$$\tan 2\theta = \frac{m_{32}\cos 2\psi_1 + m_{13}\cos 2\psi_2 + m_{21}\cos 2\psi_3}{-(m_{32}\sin 2\psi_1 + m_{13}\sin 2\psi_2 + m_{21}\sin 2\psi_3)}$$

$$\frac{r^2}{1-r^2} = \frac{m_1\cos^2(\psi_2-\theta) - m_2\cos^2(\psi_1-\theta)}{m_{21}}$$

$$b^2 = \frac{\frac{3}{2}\left[\frac{1}{r^2} + 1\right]}{m_1+m_2+m_3} \quad , \quad a^2 = b^2r^2 \qquad \ldots(D.9)$$

The drift velocity is found from equation D.6 for i=1,2.

$$\tan(\phi - \theta) = \frac{t_1d_2\cos(\psi_2-\theta) - t_2d_1\cos(\psi_1-\theta)}{t_2d_1\sin(\psi_1-\theta) - t_1d_2\sin(\psi_2-\theta)}\left(\frac{b^2}{a^2}\right) \qquad \ldots(D.10)$$

$$V = \frac{Qt_1}{d_1\left[\frac{\cos(\phi-\theta)\cos(\psi_1-\theta)}{a^2} + \frac{\sin(\phi-\theta)\sin(\psi_1-\theta)}{b^2}\right]} \qquad \ldots(D.11)$$

where $t_1=t_{max_1}$. Then c is found from equation D.1:

$$c = \sqrt{\frac{1}{Q - V^2\left[\frac{\cos^2(\phi-\theta)}{a^2} + \frac{\sin^2(\phi-\theta)}{b^2}\right]}} \qquad \ldots(D.12)$$

D.3 Practical application

In practice, the N.T.D. is never exactly zero. The method, as applied to the winter 1976 data (section 5.5), was as follows. Only the maximum peaks in each cross correlation were available, and so selection of data required that the N.T.D. be less than 0.3. Then a weighted least squares fit to the times (similar to the least squares fit in section 3.3.3) was done to get the best apparent velocity vector. This was translated back into time delays, for which the N.T.D. is zero, and the original values of ρ_{max} were used. The value of the mean auto correlation at one lag gave the value of Q in D.4. This latter piece of data was the most inaccurate, but it was available on previous output. It would be better to use the lag for $\rho \sim 0.5$, since this is more representative of the width.

An example appears in Table D.1 (starting with N.T.D.=0).

D.4 Application to Ottawa data

This section compares pattern parameters, drift values, and quality betwen the FCA method described in Appendix C (except that the weighted fit mentioned in section C.6 is used) with those of the PMFCA described in the previous sections (except that a better estimate of the width of the mean auto correlation, as described in section D.3, is used). PMFCA values might be expected to be more similar to those of the weighted fit FCA than the unweighted, because in the latter case the heaviest weight is placed on the peak value, whereas the PMFCA just uses the peak value. Comparisons of quality will demonstrate the difference between using single points (PMFCA) to represent the correlations, and the presumably better statistical fit to the peaks (wt'd FCA). Differences between wind values and pattern parameters may indicate the extent to which the Gaussian assumption applies (e.g. the assumption that the widths of all correlation peaks are equal); however, this is rather difficult to separate from practical differences in the methods. For example, if the weighted fit is made over a 'double peak' in the cross correlations indicating either a spurious peak close to a wanted peak, or an average over two pattern motions, the peak widths will tend to be greater in the final fitted solution than those found by the PMFCA (which are based only on the width of the auto correlation). This would presumably lead to systematic differences between the two methods.

Figure D.2 shows a comparison of pattern parameters. The possible bias just mentioned seems to be present, i.e. pattern scales and characteristic time are smaller for the PMFCA, as would be expected from thinner cross correlation peaks (see Appendix E). The median off-$\perp$ angle is shown for all axial ratios. This parameter had also been examined for large and small ratios (divided along 1.3), with the result that the smaller ratios showed a little less perpendicularity, but still were certainly not random. The large value of off-$\perp$ angle at low heights seems to suggest a preferred direction of elongation ($\sim$N-S) here. It should be noted that, with such a small amount of data taken at noon (Feb 4,7 1975), the velocity vectors are liable to be approximately the same at a given height, so that a preferred pattern orientation would also show up as a preferred off-$\perp$ angle (although not necessarily small). It is felt, however, that perpendicular alignment is probably the more realistic conclusion (except at low heights), since this has also been found in U of S data.

Table D.2 compares the quality of FCA (wt'd) and PMFCA values, and also the speed ratio and direction differences. The quantity of PMFCA data (not shown) was about 10% less than that from the FCA (wt'd) analysis. The reason for this is at least partly the large lag step (1 sec) in relation to the fading rate, resulting in very sharp correlation peaks at times, with only one or two values greater than 0.1. This makes accurate location of the peak position and value to be used in PMFCA

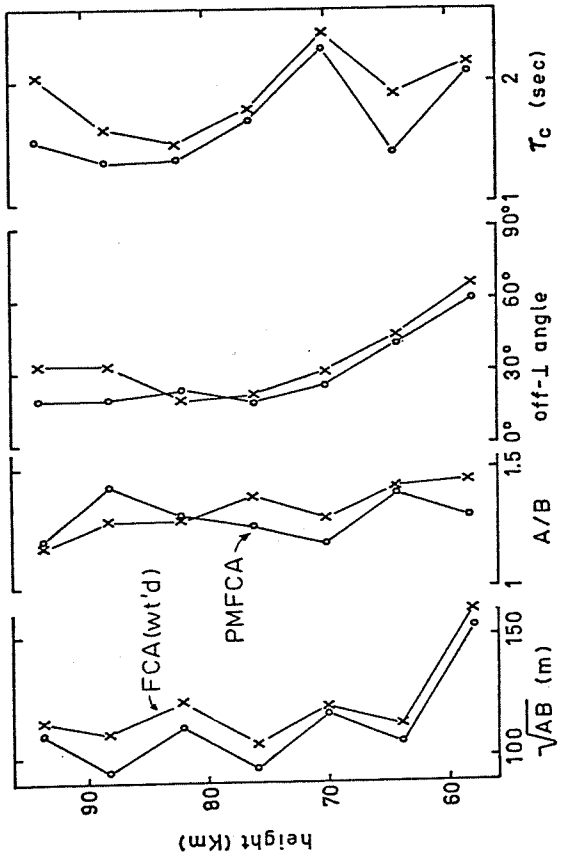

Figure D.2 Comparison between median pattern parameters from the least squares fit method (Appendix C), FCA(wt'd); and the PMFCA method, on Ottawa data (winter, noon).

Table D.2 Comparison of quality and drift values between FCA (wt'd) and PMFCA analyses(C.R.C. data).

height range	Quality: Adj. hts. % occurrence $\Delta\phi<20^\circ$	Quality: Adj. hts. % occurrence $\Delta V/V<20\%$	Quality: Adj. times % occurrence $\Delta\phi<20^\circ$	Quality: Adj. times % occurrence $\Delta V/V<20\%$	median $\frac{V_{FCA}}{V_{PMFCA}}$	% occurrence $\lvert\phi_{FCA}-\phi_{PMFCA}\rvert < 10^\circ$
all hts.						
FCA(wt'd)	69	86	73	63	0.925	77
PMFCA	76	94	90	82		
58-80Km						
FCA(wt'd)	82	87	78	72	0.91	83
PMFCA	87	93	92	91		
80-98Km						
FCA(wt'd)	50	84	63	47	0.91	69
PMFCA	57	96	87	64		

difficult, and was not done in these cases.

It can be seen that the PMFCA gives better, sometimes much better, quality; although both data sets show very good quality when compared with U of S data. The median value of the speed ratio shows that PMFCA gives generally larger values of speed. The upper and lower quartiles for this ratio (all heights) were 0.99 and 0.84. Again this can be explained in terms of systematic differences in the widths found for the correlation peaks. A similar difference in speeds had been found in Appendix B when unweighted and weighted least squares fits had been compared.

The directions agree very well, but better at low heights. The reason for the better quality of the PMFCA may be, as stated before, that sometimes the FCA method includes spurious peaks to the side of the primary peak in the fit.

APPENDIX E

STATISTICAL BIASES IN FCA PARAMETERS DUE TO SYSTEMATIC EFFECTS

E.1 Introduction

Two possible biases in analysis and results have already be briefly mentioned. One is the reduction in the peak cross correlation values if two simultaneous independent pattern motions contribute to the fading data, and the peaks for one of the motions are selected (through the NTD) for analysis. A change in pattern motion during the record is also in this category. It is possible that most records exhibiting several well defined motions would be rejected because the chosen peaks would not all come from the same motion, and the NTD would not be close enough to zero to pass this criterion.

The other is that the existence of 'spurious' peaks near the 'correct' ones (or widening of peaks due to minor changes in velocity) may bias the least squares fit method (Appendix C) to larger correlation peak widths than are actually caused by the pattern motion. This would not affect the PMFCA method seriously, unless the peaks were almost superimposed, since only the maxima are used, not the full peaks. It is possible that large 'spurious' peaks could also affect the values of the maxima, however.

'Artificial' biases of this latter type can also be caused by data filtering, which is discussed in section E.4.

Since the peak widths and maximum values are just those parameters used in the PMFCA method, the resulting biases are most easily tested with this method.

E.2 Simultaneous pattern motions.

Severe restrictions have to be placed on fading models in order to get numerical results without actually generating fading sequences; however, the general features should apply to real data.

Firstly, assume a simultaneous two pattern situation in which the mean, s.d., and auto correlation due to each pattern alone are equal, but the fading due to each is independent of the other. Since amplitudes are being correlated, it must be assumed that they add to give the measured signal; otherwise the problem becomes non-linear. This is an incorrect assumption, since there will be (random) phase differences between the two signals. It is also assumed that the motions are sufficiently different that the cross correlation peaks due to each are not modified unduly (overlapped) by those those from the other. It is easy to show that the resulting auto correlation is not changed, and that the cross correlations at any lag, τ, are given by the average of those from each pattern motion at the same lag. Thus, for this particular situation, the magnitudes of the peaks will be reduced by a factor of two, and the positions of the peaks in lag will be virtually unaffected. Of course, if there is peak overlap between the two patterns, the problem becomes very complicated, since both the determined peak positions and values will be modified; however, it it is possible that a high value of NTD would be obtained and cause rejection of the data.

In any case, the effect of reducing the cross correlation peaks by a constant factor without modifying their positions

has been investigated by taking sets of FCA parameters from the realistic random distributions in Chapter 6 (eqn. 6.4). The values used by the PMFCA (Appendix D), ρ_a, t_{max_i}, ρ_{max_i}, i=1,2,3 (t_a was chosen to be 1 sec) were calculated from these assuming an antenna spacing of 169 m. Then the values of ρ_{max_i} were divided by 2, and the modified FCA parameters calculated. Histograms of ratios of modified (primed) to original parameters are shown in Figure E.1; angle differences are shown directly. The tilt angle is not shown since it is unchanged by the process. However, the off-$\perp$ angle was found to be smaller in every instance, viz. the modified drift direction was more perpendicular to the direction of elongation than the original. As might be expected, the modified pattern scale is smaller, accounting for the reduced cross correlations. The speed is modified quite severely towards lower values, but the drift direction is only changed by a small amount.

E.3 Increased peak widths due to differences in analysis.

In this case, the modification to the original correlations is made by dividing ρ_a by 2. This represents a <u>reduction</u> in peak half widths by ~20-50%, depending on the initial parameters. Under the Gaussian correlation assumption the widths of auto and cross correlation peaks are equal (see Chapter 3, section 3.4.6), and so this modification effectively reduces all widths alike. The same distributions of initial FCA parameters is used. The drift direction is not changed by the modification. The results are shown in Figure E.2. Increases occur in speed and

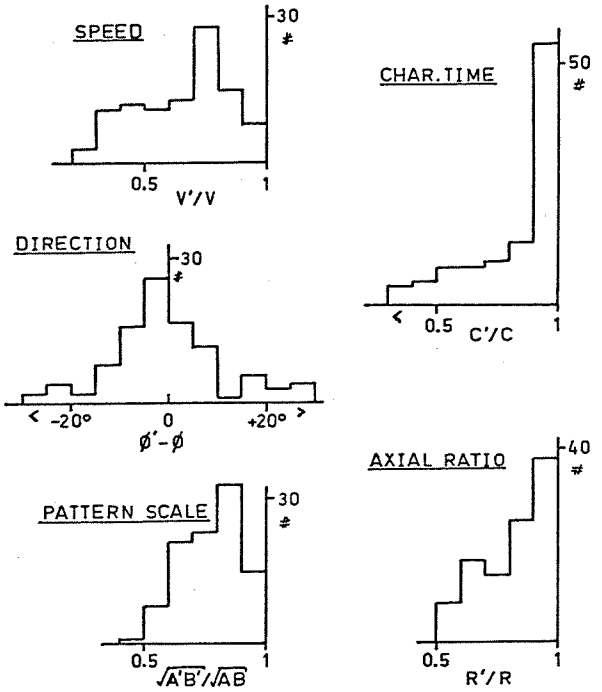

Figure E.1 Effect on FCA parameters of a reduction in the peak cross correlation values by a factor of 2. Modified values are primed.

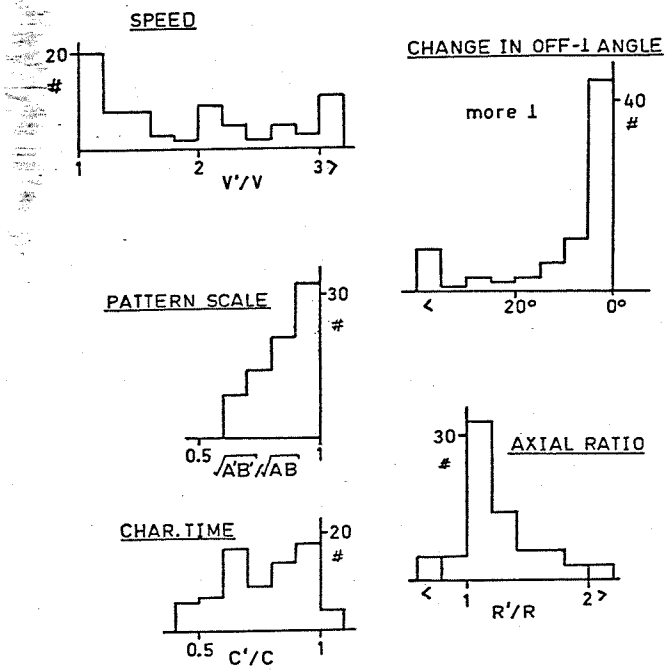

Figure E.2 Effect of FCA parameters of a reduction in the width of the correlation peaks (The auto correlation value at 1 lag, =1 sec, has been divided by 2). Modified values are primed.

axial ratio, and decreases in pattern scale and characteristic time. An interesting effect is that the direction of elongation becomes more perpendicular to the drift direction in every instance.

If there is a bias to wider peaks in the FCA least squares fit method due to spurious side peaks (or other reasons, possibly related to the applicability of the Gaussian assumption), then this method should correspond to the unmodified parameters, and the modified parameters correspond to the PMFCA method. Thus, the PMFCA, when used on real data, should show greater speed and axial ratio, smaller pattern scales and characteristic time, and a lower off-⊥ angle on the average. This comparison was done in Appendix D (section D.4), and supports these expectations (except for axial ratio which only agrees at the greater heights). So apparently, for analysis or other reasons, the width of the auto correlation is generally smaller than the widths of the cross correlations.

E.4 Data filtering.

Since systematic modification of the correlations is just what occurs under data averaging, or other filtering, the same procedure may be used to numerically evaluate the effect of filtering on the calculated FCA parameters.

Chandra and Briggs (1976) have shown theoretically that filtering fading data is equivalent to a convolution of the auto and cross correlations with the 'squared' (i.e. convolved with itself) time domain filter, which are renormalized to make the auto correlation equal to 1 at zero lag. If the time domain filter is

$$w(t) = a \exp(-\frac{t^2}{2\sigma_f^2}) \qquad ...(E.1)$$

then the squared filter is

$$w^2(t) = a' \exp(-\frac{t^2}{2(2\sigma_f^2)}) \qquad ...(E.2)$$

where the factors a, and a' are not important. The 'width' of the filter is $2\sigma_f$, and is a measure of the cutoff frequency (low pass) which will be defined arbitrarily as $f_c=1/(2\sigma_f)$.

Chandra and Briggs have also shown that, if the basic assumptions for FCA are met (i.e. ellipsoidal surfaces of constant correlation in X,Y,t space), then the values and positions of the maxima in the cross correlations are not changed by filtering. What does change is the width. If Gaussian correlations are assumed, then the modified correlations are given by

$$\rho(\tau) = \rho_{max} \exp\left[-\frac{(\tau-t_{max})^2}{2(\sigma^2+2\sigma_f^2)}\right] \qquad ...(E.3)$$

(the modified auto correlation is given from this by setting $\rho_{max}=1$, $t_{max}=0$), where the filter w(t) in equation E.1 has been used.

It appears that data, of originally Gaussian nature, on

which a high pass filter has been used, does not remain Gaussian. It is fairly easy to prove this with the high pass filter 1-w(t), but may be difficult in general. It would also be of interest to see whether surfaces of constant correlation remain ellipsoidal.

However, without creating model fading sequences, the effect of high pass filtering may be inferred by reducing the widths of the correlations according to

$$\rho(\tau) = \rho_{max} \exp\left[-\frac{(\tau-t_{max})^2}{2(\sigma^2-2\sigma_f^2)}\right] \qquad ...(E.4)$$

This in effect increases the high frequency content (i.e. flattens the spectrum). Since the original widths of the correlations are determined by the initial FCA parameters, there will be some cases where this process will create a 'negative' width, and it will be impossible to calculate the modified FCA parameters. Note that σ_f is not now related to a 'cutoff' frequency, but it is still a convenient parameter for specifying the modification of the data.

A statistical analysis has been done as in previous sections by taking random sets of FCA parameters, modifying the corresponding correlations (in this case just the width) and calculating the modified FCA parameters from these. Figure E.3 shows the relation between modified (primed) and original parameters. The right side of the figure shows the effect of a true low pass filter, the left side, the result of increased high frequency content. 100 sets of random FCA parameters were used for each filter size. Solid lines connect the medians, and bars show upper and lower quartiles. The values on the left hand side

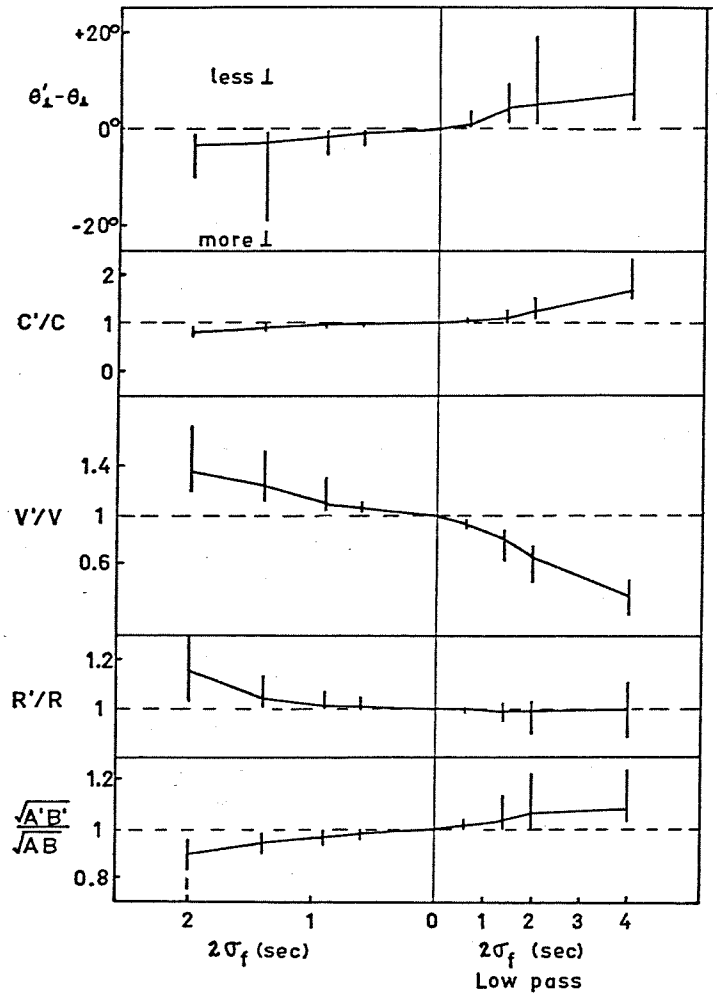

Figure E.3 Effect of data filtering on FCA parameters (modified values are primed). Left panel shows the effect of increasing the high frequency content of the record. Right panel represents a true low pass filter (which approximates a block data filter of width $2\sigma_f$). Solid lines join median values. Bars indicate upper and lower quartiles.

do not represent the full 100 calculations, since sometimes data modification produced an impossible situation (i.e. imaginary pattern parameters) as discussed previously. This occurred 50% of the time for the far left 'filter' size.

The results indicate that small amounts of data averaging should have virtually no effect on the magnitudes of FCA parameters, and the changes noted with varying amounts of averaging in Appendix B must be due to some other cause, possibly the change in lag step. It has been tacitly assumed here that the Gaussian weight filter is approximately the same as a block filter of width $2\sigma_f$. The maximum amount of averaging which has been done on U of S data, in routine processing, is $2\sigma_f$= 0.6 sec.